B.A.R.C.-291

206

INDC(IND)-001/G

B.A.R.C.-291

'सत्यमेव जयते'

GOVERNMENT OF INDIA
ATOMIC ENERGY COMMISSION

VAN DE GRAAFF LABORATORY PROGRESS REPORT

Compiled by
T. P. David
Nuclear Physics Division

BHABHA ATOMIC RESEARCH CENTRE
BOMBAY, INDIA
1967

B.A.R.C. - 291

GOVERNMENT OF INDIA
ATOMIC ENERGY COMMISSION

B.A.R.C.-291

VAN DE GRAAFF LABORATORY PROGRESS REPORT

Compiled by

T.P. David
Nuclear Physics Division

BHABHA ATOMIC RESEARCH CENTRE
BOMBAY, INDIA
1967.

CONTENTS

	Page
Introduction	1
Accelerator	2
Research Experiments	9
Instrumentation and data processing	41
Radiation Survey	45
Seminars	46
Indian Nuclear Data Group	47
Library	48

INTRODUCTION

This report covers the operation and utilization of the 5.5 MeV Van de Graaff accelerator at Trombay during the year 1966, the fifth year of the accelerator operation. Throughout this period the accelerator has been worked on round the clock basis.

The ion sources reprocessed in the laboratory have been in use since November 1965 and these have given satisfactory and fairly long service. By the end of 1966 the accelerating tube has been working for more than 22,000 hours.

Experiments with charged particle reactions for the study of nuclear structure and nuclear reactions as well as angular correlation experiments have been continued[1]. A number of research experiments have been carried out during the year and are reported under the section on research experiments.

A chart showing the machine availability for research experiments giving the time loss due to breakdowns during the 5 year period of its operation has been included.

1) Van de Graaff Progress Report T.P. David, AEET 254 (1966).

ACCELERATOR

I. Analysis of Accelerator operation during the period.

Machine run

1.	Total time available from 1st January to 31st December, 1966 ..	8760 Hours
2.	Holiday observed during the year	24 Hours
3.	Time used for routine maintenance	624 Hours
4.	Other maintenance work	168 Hours
5.	Shut down due to power and water failure	190 Hours
6.	Maintenance work (including rewiring) on chiller and Air conditioning plant.	288 Hours
7.	Number of hours Accelerator run	5780 Hours
8.	Time lost due to breakdowns	1686*Hours
		8760 Hours

Machine utilization

1.	Time used by research groups	4844 Hours
2.	Time used for conditioning the machine	593 Hours
3.	Time used to check machine calibration	96 Hours
4.	Time lost due to failure of experimental facilities	247 Hours
		5780 Hours

---

* 660 hours have been spent for transfer of insulating gas and accelerator tank roughing.

II. <u>Component replacements:</u>

1. Ion source bottles are being regularly reprocessed in the Laboratory[1]. These reprocessed ion sources have been used in the accelerator from November 1965 and have given excellent service. The aluminium canals which are renewed every time the sources are reprocessed, are fabricated in the Nuclear Physics Workshop. Extreme care is taken in the fabrication of these canals as even a very minute error in the canal axis is found to cause an undesirable shift of the beam position at the defining slits above the analyzing magnet. A total of 9 reprocessed ion sources have been used during the year giving an average service of 640 hours each.

2. Thermomechanical leaks for use in the gas feed line to the accelerator ion source bottle are fabricated in the laboratory[2]. Stainless steel cylinders are now used instead of brass as these are found to give longer service before developing any cold leak. The thermomechanical leaks have been renewed 4 times during the period under report.

3. A number of small components such as high voltage bushings and corona collector units are now fabricated in the laboratory for replacements.

1) Van de Graaff Laboratory Progress Report - T.P. David AEET 254(1966) 6.
2) Van de Graaff Laboratory Progress Report - T.P. David AEET 214 (1965) 10.

III. Modifications and additions:

1. Fabrication and assembly of one more pair of electromagnetic quadrupole focusing lenses with an aperture of 2.5 cms have been completed. This has been installed in one of the side ports of the switching magnet and has been working satisfactorily. More such quadrupole lenses are under fabrication.

2. Isolation valves have been fitted with all the vacuum gauges in the accelerating and differential tubes.

3. A liquid nitrogen trap suitable for installation between the main and booster diffusion pumps of the accelerator vacuum system has been designed and fabricated. The trap is undergoing vacuum test prior to installation.

4. Selsyn motors driving the terminal control cords have been a constant source of trouble necessitating the opening of the accelerator tank for repairs. It is planned to replace these systems with reversible geared DC motors. A prototype with push button operation incorporating limit switches and indicating lamps has been constructed and tested. Several such units are under fabrication. The replacement is to be carried out in the immediate future.

IV Accelerator breakdowns:

Most of the time lost in breakdowns has been due to the failure of the various electrical and electronic components as can be seen from the table given below. A few more of the accelerating tube glass sections have developed cracks due to heavy sparking and these sections are electrically shorted to avoid further damage. The total number of sections thus shorted are 12 in the upper and 2 in the lower tube sections. However, no apparent change in the beam focusing characteristics has been so far observed in the working of the accelerator due to this shorting of accelerating sections.

Component	Failure during the year (Number of times)
1. Selsyn motors	9
2. Column resistors	10
3. Column spring	3
4. Charging resistor	1
5. N.M.R. Power supply	2
6. Focus supply series resistor	1
7. Belt charge supply	3
8. Analysing magnet supply	4
9. Balance amplifier	7
10. Corona assembly	7
11. Switching magnet supply	1
12. Terminal high voltage bushing	2
13. Accelerator vacuum system	1
14. Auxiliary vacuum system	1
15. Corona collector replacement	4

Failure of the components may be attributed to the high humidity in the accelerator room, beam room and control room, particularly during the monsoon months. Attempts are being made to improve the air conditioning system to take care of humidity control.

V. Operation Analysis - Five year period:

A month to month analysis of accelerator operation during the last five years has been made. Fig. (1) gives the time the accelerator was utilized for research experiments as a percentage of the maximum possible experimental time without breakdowns.

VI. Development project:

1. Five port switching magnet[12] T.P. David, N. Sarma, M. Bhatia and P.R. Sunder Rao - The magnet yoke and pole pieces have been fabricated from Tata 'A' grade steel and assembled. A magnet mount has been designed and fabricated with provision for levelling and for movement of the magnet by $\pm$ 1.5 cms in the direction perpendicular to the beam axis. The magnet coil has been fabricated from electrical grade aluminium tubing of 12.7 mm square section. Insulation between the turns has been provided by winding PVC insulation tape over the tube throughout its length. The coil was made in units of double layers of 11 turns each and taped. These units are assembled on the pole pieces and welded end-to-end to maintain continuity of current as well as the flow of cooling water. A high current variable DC supply has been built for feeding the main coils. This supply is stabilized by a bank of series controlled transistors. The stabilization unit has been built by the Technical Physics Division.

It is proposed to provide each exit port with a pair of adjustable insulated pick up slits. The amplified signals picked up by these slits would control a low current power supply feeding an

FIG-1

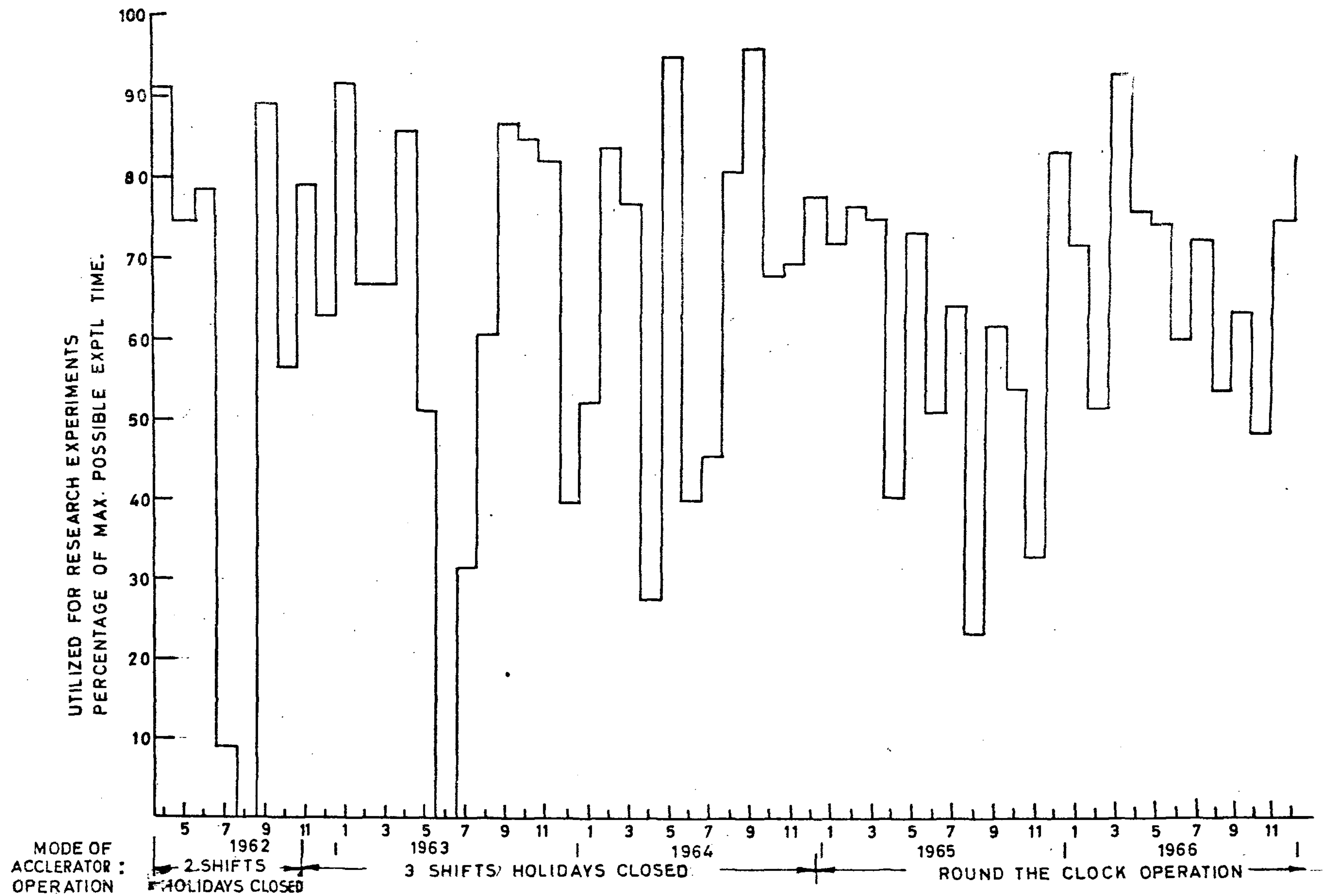
UTILIZED FOR RESEARCH EXPERIMENTS
PERCENTAGE OF MAX. POSSIBLE EXPTL TIME.
100
90
80
70
60
50
40
30
20
10
5 7 9 11 1 3 5 7 9 11 1 3 5 7 9 11 1 3 5 7 9 11 1 3 5 7 9 11
1962
1963
1964
1965
1966
MODE OF ACCLERATOR OPERATION :
2 SHIFTS HOLIDAYS CLOSED
3 SHIFTS/ HOLIDAYS CLOSED
ROUND THE CLOCK OPERATION

lens system are under test. It would be quite interesting to study the effect of such a system just below the ion source because it requires less voltage, minimizing insulation and power supply miniaturization problems.

1) Van de Graaff Laboratory Progress Report - T.P. David AEET - 254 (1966).

RESEARCH EXPERIMENTS

1. Total Cross Section for the reaction $^{51}V(p,n)^{51}Cr$ - K.K. Sekharan, M.K. Mehta and A.S. Divatia - The total neutron yield for the $^{51}V(p,n)^{51}Cr$ reaction has been measured in the incident proton energy range 1.56 to 5.53 MeV using a 4π neutron counter. A thin Vanadium metal target evaporated on to a thick tantalum backing was bombarded with protons, the incident protons being monitored by a current integrator. The step in which the yield was measured varied from 6 to 10 KeV. The excitation function a part of which is shown in figure 2 shows a number of peaks which are overlapping. The dots are the total cross section values obtained by a separate measurement using a thick target.

$^{51}V+p$ in the incident energy range 1.56 to 5.53 MeV leads to an excitation energy of about 12 to 16 MeV in the compound nucleus ^{52}Cr which is the statistical region. The data was, therefore, analyzed on the basis of the fluctuation theory. Since the neutron yield increases rapidly with the incident energy the data was split into three ranges of energy namely 1.56 - 2.55, 2.55 - 3.84 and 3.84 - 5.53 MeV. The auto correlation function $C(\epsilon)$ was evaluated using the equation.

$$C(\epsilon) = \frac{\Delta E}{E_2 - E_1} \sum_{E_1}^{E_2} \left(\frac{\sigma(E_i)}{<\sigma(E_i)>} - 1 \right) \left(\frac{\sigma(E_i + \epsilon)}{<\sigma(E_i + \epsilon)>} - 1 \right)$$

for the three energy ranges separately for various values of the averaging interval, δ. In figure 3 C(0) is shown as a function of δ for the three energy ranges. C(0) remains constant for a certain range of values of δ for all the three curves. Averaging interval is chosen from this range for evaluating the average width, Γ. In the upper portion of figure 2, $C(\epsilon)$ against small values of ϵ is plotted for averaging intervals equal to 225, 313, 237, 345, 304 and 378 KeV. Crosses are the experimental points. The dots are the calculated values using the formula $C(\epsilon) = C(0)\frac{\Gamma^2}{\Gamma^2+\epsilon^2}$ where Γ is the average level width. Since the energy step in which the neutron yield is measured is large compared to the average width obtained there are only two or three experimental points which lie on the Lorentzian. Since there are only two or three points on the curve error as much as $\pm$ 50% of Γ could be assigned to the value of Γ though the F.R.D. error is much smaller.

In the present experiment the experimental resolution ρ is about 1.5 KeV which is less than the average width Γ and the energy step ΔE. In an ideal case for which fluctuation analysis is applied ρ and ΔE should be less than Γ. Corti et. al.[1] have developed a method of extracting Γ where $\Gamma < \rho$. For applying this method a necessary condition is that E should be equal to ρ. In the present experiment since ρ is less than ΔE Corti's method was not applied.

The average width Γ obtained for levels in the ^{52}Cr nucleus in the excitation energy range 12 to 16 MeV is 3.5 KeV.

1) M. Corti, M.G. Marcazzan, L. Milazzo Colli and M. Milazzo, Energia Nucleare, 13, (1966) 312.

2. <u>Study of levels in ^{28}Si</u> - S.S. Kerekatte, A.S. Divatia, M.K. Mehta, K.B. Nambiar and K.K. Sekharan - Some excited levels in ^{28}Si, lying in the 14 MeV region, have been studied by the technique of elastic scattering of alpha particles by ^{24}Mg. The

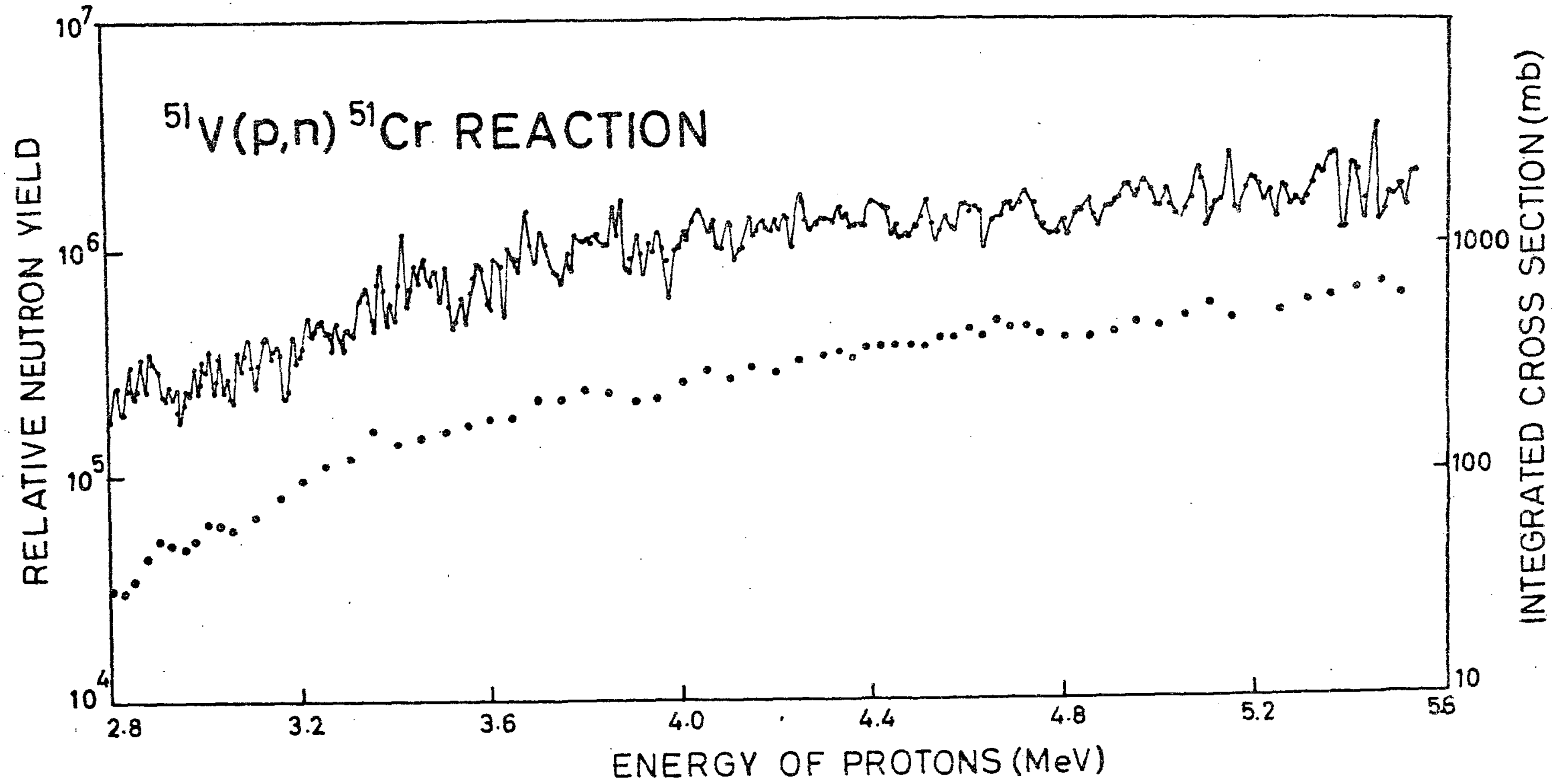

$^{51}V(p,n)^{51}Cr$ REACTION
RELATIVE NEUTRON YIELD
10^7
10^6
10^5
10^4
INTEGRATED CROSS SECTION (mb)
1000
100
10
2.8
3.2
3.6
4.0
4.4
4.8
5.2
5.6
ENERGY OF PROTONS (MeV)

FIG·2

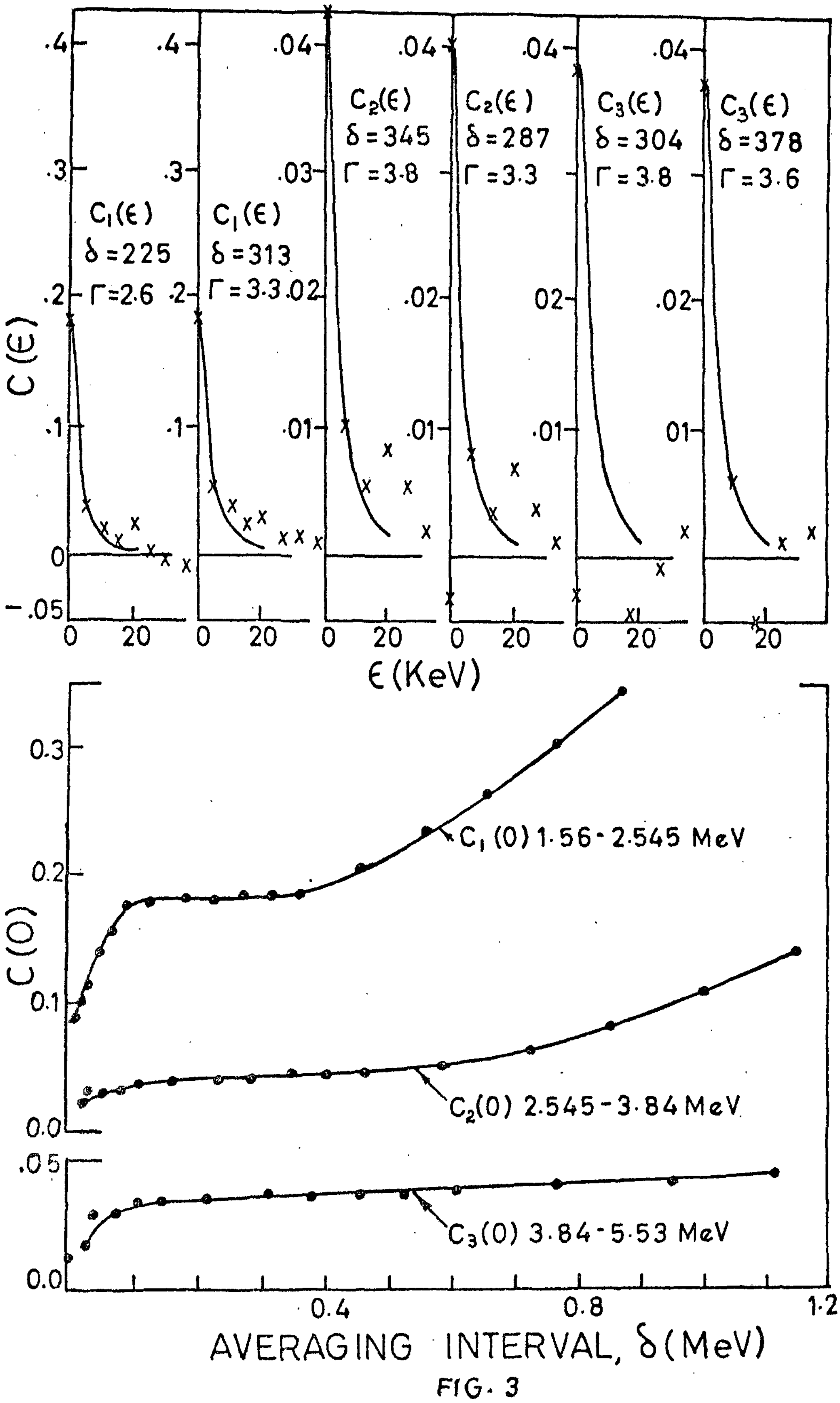

C₁(ε) δ=225 Γ=2.6
C₁(ε) δ=313 Γ=3.3
C₂(ε) δ=345 Γ=3.8
C₂(ε) δ=287 Γ=3.3
C₃(ε) δ=304 Γ=3.8
C₃(ε) δ=378 Γ=3.6
C(ε)
ε (KeV)
C(0)
C₁(0) 1.56-2.545 MeV
C₂(0) 2.545-3.84 MeV
C₃(0) 3.84-5.53 MeV
AVERAGING INTERVAL, δ (MeV)

FIG. 3

analysis will be done in order to confirm the spin and parity assignments, and to obtain the resonance parameters.

1) S.S. Kerekatte, et al, Proc. Nucl. Phys. & Sol. State Phys.,Symp., Bombay (1966) 120.

3. Computer programmes for the analysis of particle-gamma ray angular correlation measurements in nuclear reactions - M.A. Eswaran - For the analysis of the particle-gamma ray angular correlation measurements in the nuclear reactions of the type X $(a, b\gamma)y$ employing the 'method II' of Litherland and Ferguson[1] a computer programme has been written in Fortran for the CDC - 3600 of T.I.F.R. According to this method, the angular correlation expression is written as a linear combination of contributions due to various magnetic substates of the level excited in the residual nucleus. Due to the special choice of $0°$ or $180°$ detection for the outgoing particles, the substates which are populated in the residual nuclear state are limited by the sum of the target spin and the spins of the bombarding and outgoing particles. The angular correlation function can be put in the following form, from the equations given in ref: (2)

$$W(\theta_\gamma) = \sum_K a^0_{K0} Q_K \sqrt{2K+1} \; P_K(\cos\theta)$$

where

$$a^0_{K0} = \sum_m P(m) \sum_{LL'} \delta^p C^0_{K0}$$

Q_K are the angular correlation attenuation factors due to the gamma counter size and δ is the quadrupole to dipole amplitude mixing ratio for the gamma ray. LL' refer to the multipolarities of the gamma ray and p = 0, 1 and 2 for LL' = 11, 12 and 22.

For each spin choice of the level the angular correlation coefficients are fed as input in the programme from the tables of Smith[2)] and a linear least squares fitting procedure is used with the magnetic substate population parameters as unknowns. The result of this fitting procedure is a value of χ^2, the weighted sum of the squares of the deviations. This procedure is repeated to cover the whole range of the quadrupole to dipole mixing amplitude ratio parameter δ. In the programme δ is taken as tan τ and χ^2 values are obtained for different values of τ from -90° to $+90^\circ$ in any desired steps. In the programme some conditional loops were included to overcome the problem of non-physical solution which may arise in the linear least squares fitting procedure when a magnetic substate population parameter turns out to be negative. When this happens, that particular parameter is suppressed to zero and the fit is repeated to get a new value of χ^2 with this constraint. Provision has also been made in the programme to investigate the effect on χ^2 of small population of higher magnetic sub-states due to finite particle counter size.

Another programme was written extending the above programme for use in the specific case of $^{26}Mg(d,p_3\gamma_1\gamma_2)^{27}Mg$ where the primary and secondary gamma rays are very close in energy that they are not resolved in the NaI gamma detector. In this case $p_3-\gamma_1$ and $p_3-\gamma_2$ with γ_1 unobserved are treated together and the combined angular correlation is analysed as described in the next section.

1) A.E. Litherland and Ferguson Can. J.Phys. 39, (1961) 788.

2) P.B. Smith in Nuclear Reactions Vol II ed. by Endt and Smith, North-Holland Publ. Co. (1962).

4. <u>Study of the 1.94 MeV state in ^{27}Mg by means of the reaction ^{26}Mg(d,pγ)^{27}Mg</u> - M.A. Eswaran, N.L. Ragoowansi and K.K. Sekharan - As a continuation[1] of the studies on the properties of the low-lying excited states in ^{27}Mg the 1.94 MeV third excited state has been studied by proton - gamma ray angular correlation measurements in the reaction ^{26}Mg(d,pγ)^{27}Mg employing the Litherland and Ferguson[2] method which is independent of any assumption regarding reaction mechanism. The experimental details are described in ref. (1). The de-excitation gamma ray spectrum in coincidence with the protons feeding the 1.94 MeV state, detected at 0° to the beam is shown in fig. 6. The angular correlation data, for the combined (0.98 + 0.96) MeV gamma ray peak due to the two transitions 1.94 $\rightarrow$ 0.98 MeV and 0.98 $\rightarrow$ 0 MeV, are plotted in Fig. 7.

This represents the sum of the following two angular correlations:

a) Angular correlation of the gamma ray due to the transition 1.94 $\rightarrow$ 0.98 MeV in coincidence with the protons feeding the 1.94 MeV state.

b) Angular correlation of the gamma ray due to the transition 0.98 $\rightarrow$ 0 MeV in coincidence with the proton feeding the 1.94 MeV state with the intermediate gamma ray due to the 1.94 $\rightarrow$ 0.98 MeV transition unobserved.

The data were analysed by a method[3] similar to the one used for 'method I' of Litherland and Ferguson. The correlation functions for (a) and (b) can be put in the following forms from the expressions quoted in ref. (4).

$$W_a(\theta_\gamma) = \sum_{\substack{m,\\ L_1 L_1'}} P_{(m)}\, \delta_1^{p_1} \sum_K C^{o}_{Ko}(J_1 J_2 L_1 L_1' m) \sqrt{2K+1}\; Q_K P_K(\cos\theta) \quad \text{-----(1)}$$

and

$$W_b(\theta_\gamma) = \sum_{L_1 L_1' L_2 L_2'} P_{(m)}\, \delta_1^{p_1} \delta_2^{p_2} \sum C^{o}_{OM}(J_1 J_2 J_3 L_1 L_1' L_2 L_2' m) \sqrt{2M+1}\; Q_M P_M(\cos\theta) \quad \text{--(2)}$$

where all the quantities are as defined in ref (4) J_1, J_2 and J_3 are the spins of the three states 1.94, 0.98 and 0 MeV of ^{27}Mg and δ_1 and δ_2 are the quadrupole to dipole mixing amplitude ratio of the first and second gamma rays due to 1.94 $\rightarrow$ 0.98 MeV and 0.98 $\rightarrow$ 0 MeV transitions respectively. P (m) is the population parameter of the magnetic substate 'm' of the 1.94 MeV state of spin J_1. The combination of two angular correlations (a)&(b) is represented by sum of the above two equations (1) & (2) i.e. $W_a(\theta_\gamma) + W_b(\theta_\gamma)$ with the constant term of each of these equations being normalized to unity.

A computer programme was written for the CDC - 3600 computer of T.I.F.R. to carry out the analysis of the data which proceeds through a linear least squares fit of the data points using the above equations with magnetic substate population parameters P (m) as the unknowns. The values of magnetic substates m are limited to 1/2 and 3/2 due to the 0^{o} detection of the protons in the reaction (2). The vector addition coefficients C^{o}_{Ko} and C^{o}_{OM} were obtained from the tables of Smith[4]. The spins J_2 and J_3 for the states 0.98 and 0 MeV are known to be[1),5)] 3/2 and

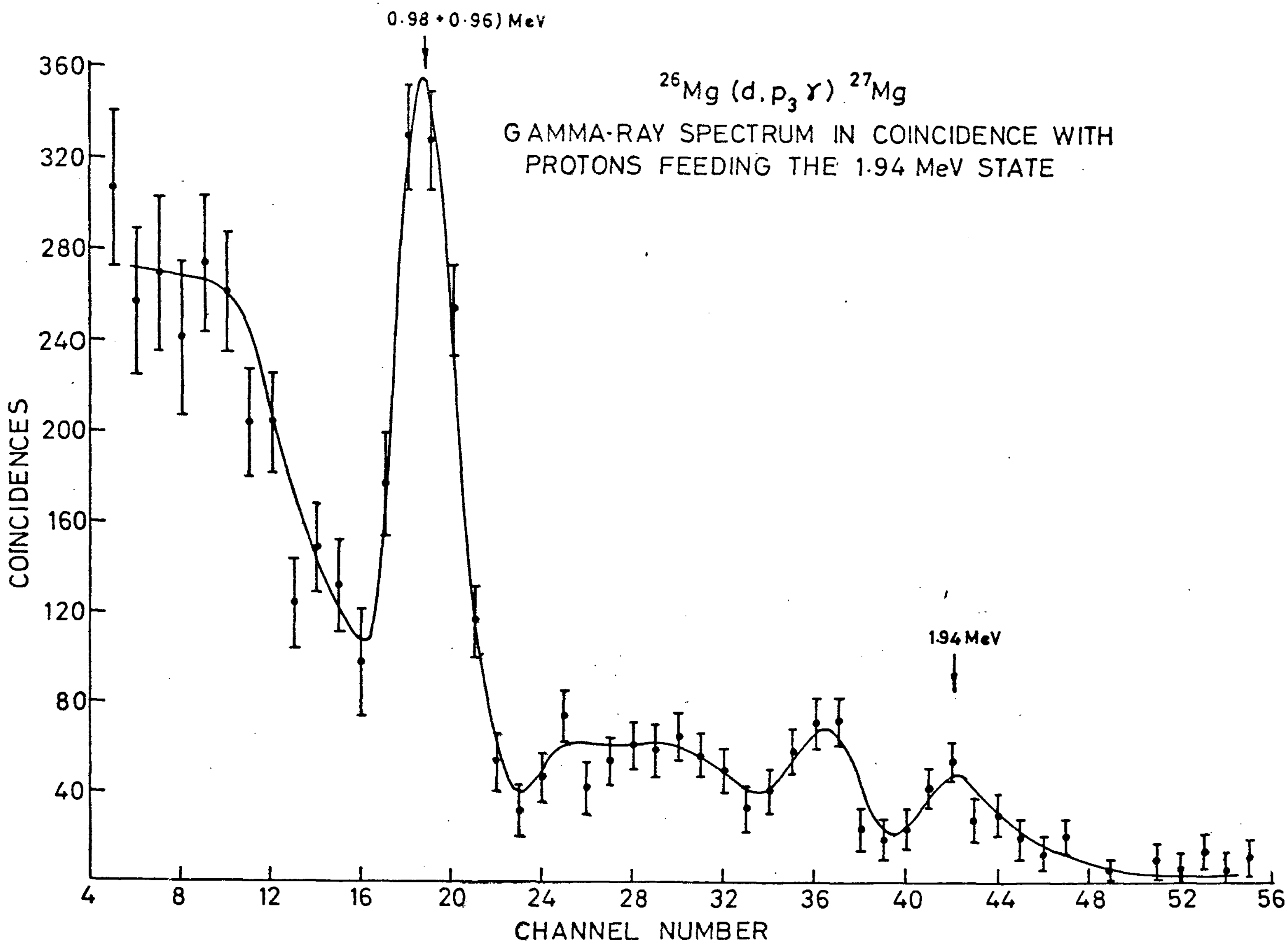

0·98 + 0·96) MeV
^{26}Mg (d, p$_3$ γ) ^{27}Mg
GAMMA-RAY SPECTRUM IN COINCIDENCE WITH
PROTONS FEEDING THE 1·94 MeV STATE
1.94 MeV
COINCIDENCES
CHANNEL NUMBER
360
320
280
240
200
160
120
80
40
4
8
12
16
20
24
28
32
36
40
44
48
52
56

FIG-6

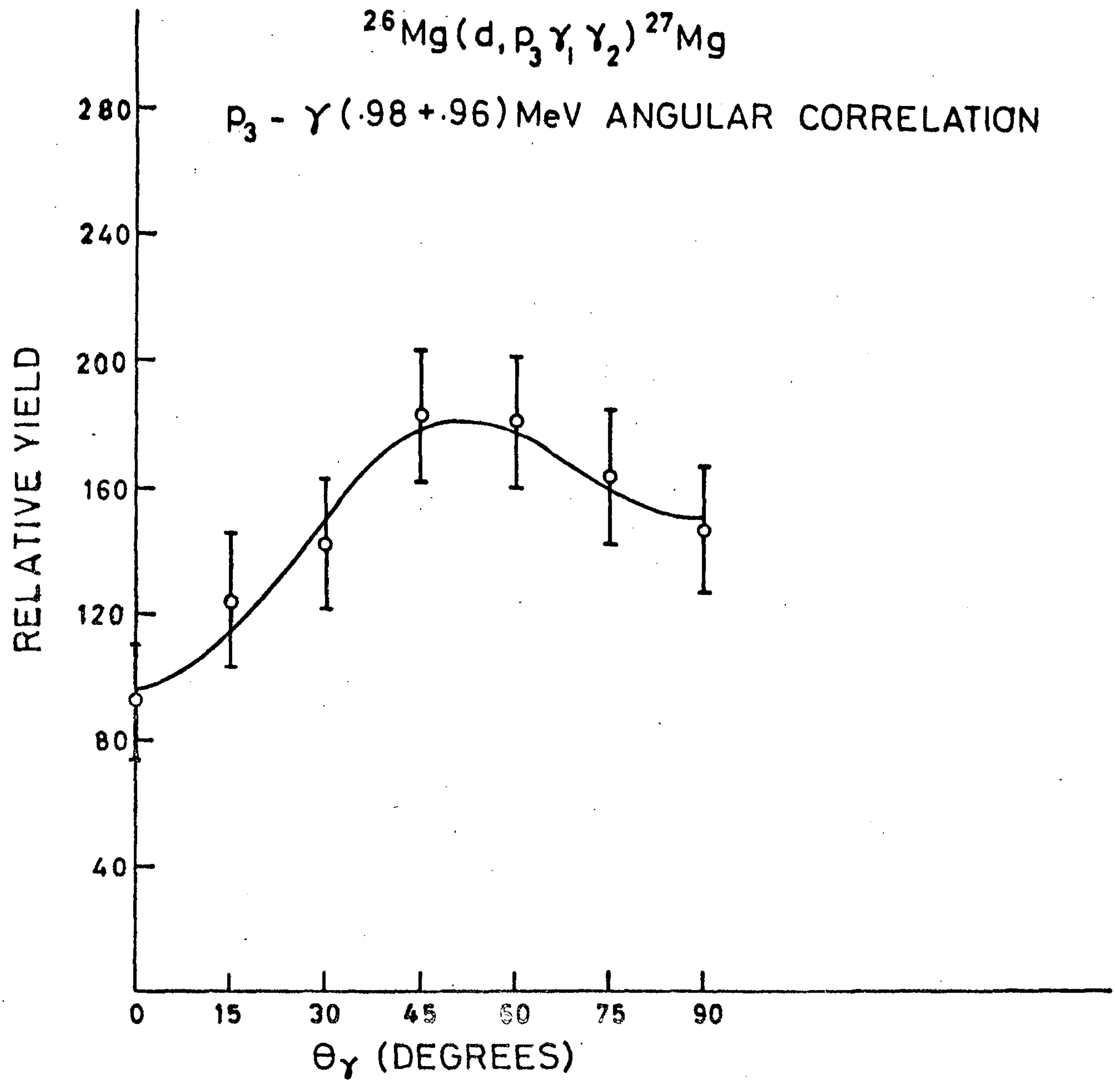

$^{26}Mg(d, p_3 \gamma_1 \gamma_2)^{27}Mg$
$p_3 - \gamma$ (·98 + ·96) MeV ANGULAR CORRELATION
280
240
200
160
120
80
40
RELATIVE YIELD
0
15
30
45
60
75
90
θ_γ (DEGREES)

FIG-7

1/2. Hence the fit is performed for a fixed spin value J_1 of the 1.94 MeV state, and for fixed values of δ_1 and δ_2. The fit is repeated over the ranges of δ_1 and δ_2 appropriate to the spin value chosen for J_1 with the multipolarities being limited to quadrupole and dipole. In the programme δ_1 and δ_2 are taken as tan τ_1 and tan τ_2 where τ_1 and τ_2 varied from $-90°$ to $+90°$ in steps of $5°$. The result of this fitting is a series of χ^2 values for various combinations of δ_1 and δ_2 for each spin choice for J_1. χ^2 is given by

$$\chi^2 = \sum_i \left[y(\theta_i) - W(\theta_i)\right]^2 / \sigma^2(\theta_i) \qquad --- (3)$$

where $\sigma(\theta_i)$ is the uncertainty assigned to the gamma ray yield $y(\theta_i)$ at angle θ_i due to counting statistics. The minima in χ^2 lead to conclusions about spin assignments. These fits were obtained for choice of 1/2, 3/2, 5/2 and 7/2 for J_1.

This analysis showed that χ^2 values were insensitive to variations in δ_2. Choosing a value[6] of 0.176 for δ_2 the χ^2 plots are shown as a function of τ_1 (= a Ω ctg. δ_1) in fig.8 for various spin choices J_1 for the 1.94 MeV state. This analysis shows that spin value of 5/2 gives the best fit for the observed correlation with fairly large quadrupole mixture in the 1.94 $\rightarrow$ 0.98 MeV transition. Hence spin of 5/2 can be assigned to the 1.94 MeV third excited state. Further measurements are planned to be made to determine conclusively the value of multipole mixing ratio of the gamma ray due to the 1.94 $\rightarrow$ 0.98 MeV transition. From the coincidence spectrum in fig.6, the cascade to cross over branching ratio of 1.94 MeV state (i.e.) $I(1.94 \rightarrow 0.98)/I(1.94 \rightarrow 0)$ is estimated to be 2.0 ± 0.3.

In conclusion it is observed that the spin sequence and level energies of the states at 0, 0.98 and 1.94 MeV are consistent with the expectation that they form the members of the ground state rotational band.

1) Proc. of N.P. and S.S.P. Symp., Bombay (1966) 144 and BARC report 276 (1967).

2) A.E. Litherland and A.J. Ferguson, Can. J. Phys. 39, (1961) 788.

3) C. Broude and M.A. Eswaran, Can. J. Phys. 42, (1964) 1300.

4) P.B. Smith in Nuclear Reactions, Vol.II ed. by P.M. Endt and P.B. Smith, North Holland Publ. Co. Amsterdam (1962) 248.

5) P.M. Endt and C. van der Leun, Nucl. Phys. 34 (1962) 1.

6) J.M. Lacambra, D.R. Tilley and N.R. Roberson Phys. Letters 20, (1966) 649.

5. <u>Proton-gamma ray angular correlation measurements in the reaction $^{24}Mg(d,p_3\gamma)^{25}Mg$</u> - M.A. Eswaran, N.L. Ragoowansi and P.C. Mitra - To obtain direct evidence for the spin of the 1.61 MeV state in ^{25}Mg, the level was excited in the reaction $^{24}Mg(d,p_3\gamma)^{25}Mg$ using 2.1 MeV deuteron beam and detecting the outgoing protons feeding the state, at 0° to the beam in an ORTEC surface barrier detector, the angular correlation of the subsequent 1.61 MeV de-excitation γ-ray was measured. Measurements were analysed by a computer programme based on the Litherland and Ferguson[1] method which is independent of any assumption regarding reaction mecahnism. Results can be fitted with a spin choice of 3/2 or 7/2 for the state. Spin value 7/2 for this 1.61 MeV state agrees with the expectation from other evidences. For this spin value the values of quadrupole

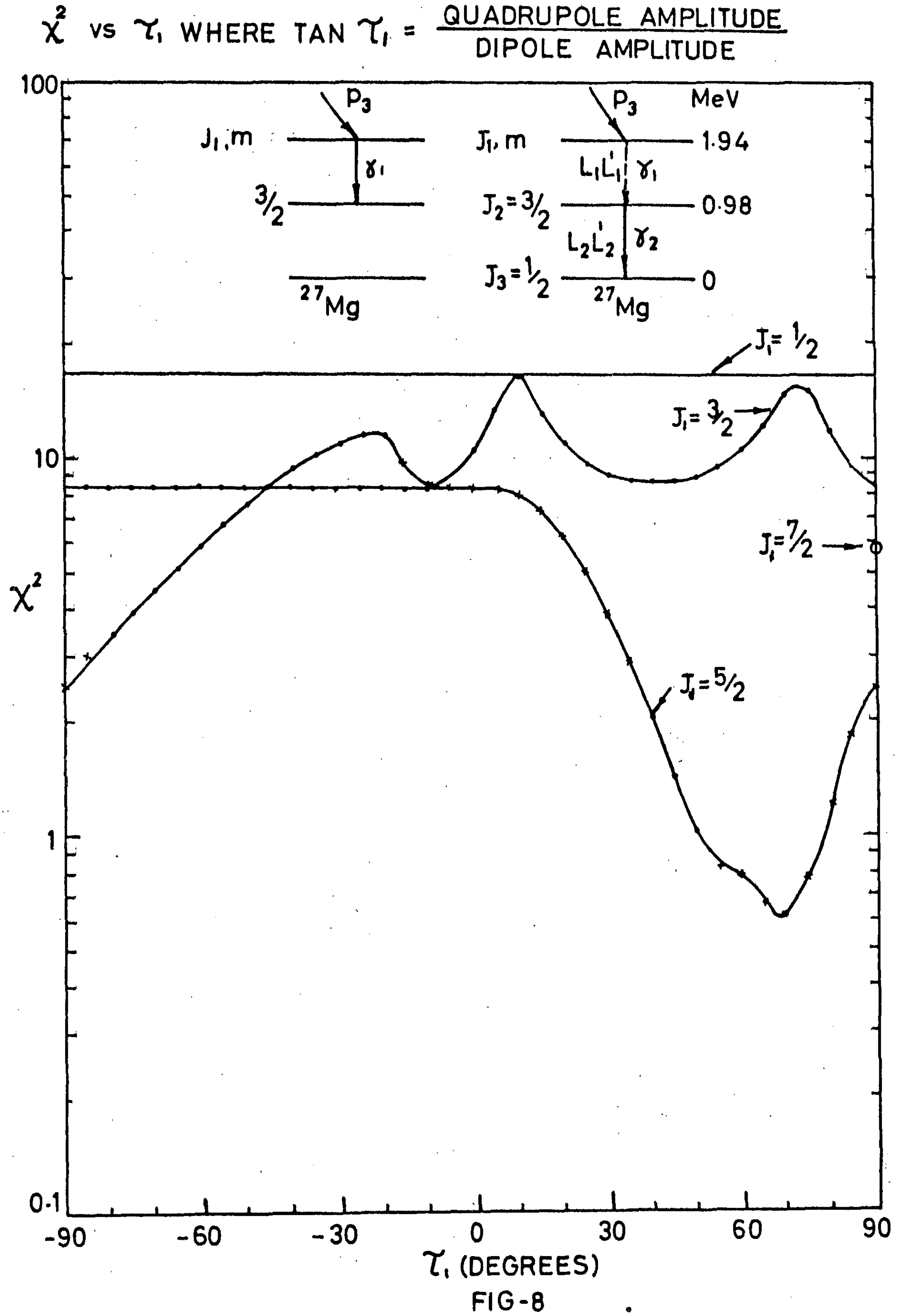

χ^2 vs τ_1 WHERE TAN τ_1 = $\frac{\text{QUADRUPOLE AMPLITUDE}}{\text{DIPOLE AMPLITUDE}}$
100
10
1
0·1
χ^2
P_3
J_1, m
γ_1
3/2
^{27}Mg
P_3
MeV
J_1, m
1·94
$L_1 L_1'$ γ_1
$J_2 = 3/2$
0·98
$L_2 L_2'$ γ_2
$J_3 = 1/2$
0
^{27}Mg
$J_1 = 1/2$
$J_1 = 3/2$
$J_1 = 7/2$
$J_1 = 5/2$
-90
-60
-30
0
30
60
90
τ_1 (DEGREES)

FIG-8

to dipole mixing amplitude ratio parameter $|\delta|$, for which the data could be fitted are 0.18 and 2.14. The value of 0.18 for $|\delta|$, is consistent with the known life time[2] of the 1.61 MeV level.

1) A.E. Litherland and A.J. Ferguson. Can. J. Phys. 39, (1961) 788
2) P.M. Endt and C. van der Leun Nucl. Phys. 34, (1962) 1.

6. <u>Fluctuation analysis of the compound nucleus levels of ^{52}Cr</u> - C.M. Lamba, N. Sarma, N.S. Thampi, D.K. Sood* and V.K. Deshpande* - A brief account of all possible aspects of the fluctuation theory as applied on the reaction elastic scattering of protons from ^{51}V [1] is presented in this work.

Excitation functions at angles (100°, 120°, 140°, 160°) covering energy range 4.005 to 5.515 in steps, δE of 5 KeV are measured with an experimental resolution Γ_0 of 1 KeV and are shown in Fig. (9). The cross section for inelastic proton and alpha groups was too small to cross background barrier.

1.1 Auto correlation analysis for full range of data. Auto-correlation functions[1] for total energy range, were calculated. It is found that $C_p(\epsilon)$ does not fluctuate about ϵ axis but has a linear modulation imposed on it. This behaviour is attributed to energy dependent non fluctuating process. In such a case the modified auto-correlation function[1] is a lorentzian displaced by an amount $K_0'(\epsilon)$ from ϵ axis (fig.10). $K_0'(0)$ is a measure of modulation. The form of $K_0'(\epsilon)$ could not be

---

* Indian Institute of Technology, Kanpur.

calculated accurately but is visually estimated to be a straight line. This shows the presence of strong modulation. The width Γ_{RAW} (ignoring modulation) and Γ_{CORR} (corrected for modulation) are shown in Table I.

The modulation effects are eliminated by taking local average of Q points of energy width $q\Gamma$. The value of q is chosen from the q dependence of $C_p^q(0)$ (fig.11). The agreement of and (Cf table I) shows that this method eliminates modulation effects. The level width Γ_q are also shown.

In Fig.9 the averaged cross section $\sigma_q(E_i)$ for $q\Gamma$ = 400 KeV and Ruthorford scattering cross sections are shown with thick and dotted lines respectively. Minimum at 4.955 MeV at all angles gives an idea of the presence of intermediate structure of width 900 KeV. However, considering that $\sigma_q(E_i)$ comprises of so many other factors, it is not possible to isolate intermediate structure.

2.1 Determination of Γ by variable energy resolution method:
The autocorrelation analysis is not a very sensitive tool when $\delta E > f$ and $\delta E > \Gamma$. As it has been made sure that $C_p(0)$ and probability histograms (section 5.1) do not vary with step size a method proposed by Corti is a more reliable tool for extracting Γ. (To ensure that two excitation function of 151 points each were constructed at each angle with δE = 10 KeV using alternate points). $C_p(f)$ the normalised variance decrease rapidly as f increases, the rate of decrease depending on Γ. By successive application of formula

$$\sigma_r(E_i) = \frac{1}{r}\sum_{\delta=i}^{\gamma=i+r-1}\sigma(E_\gamma)$$

new excitation

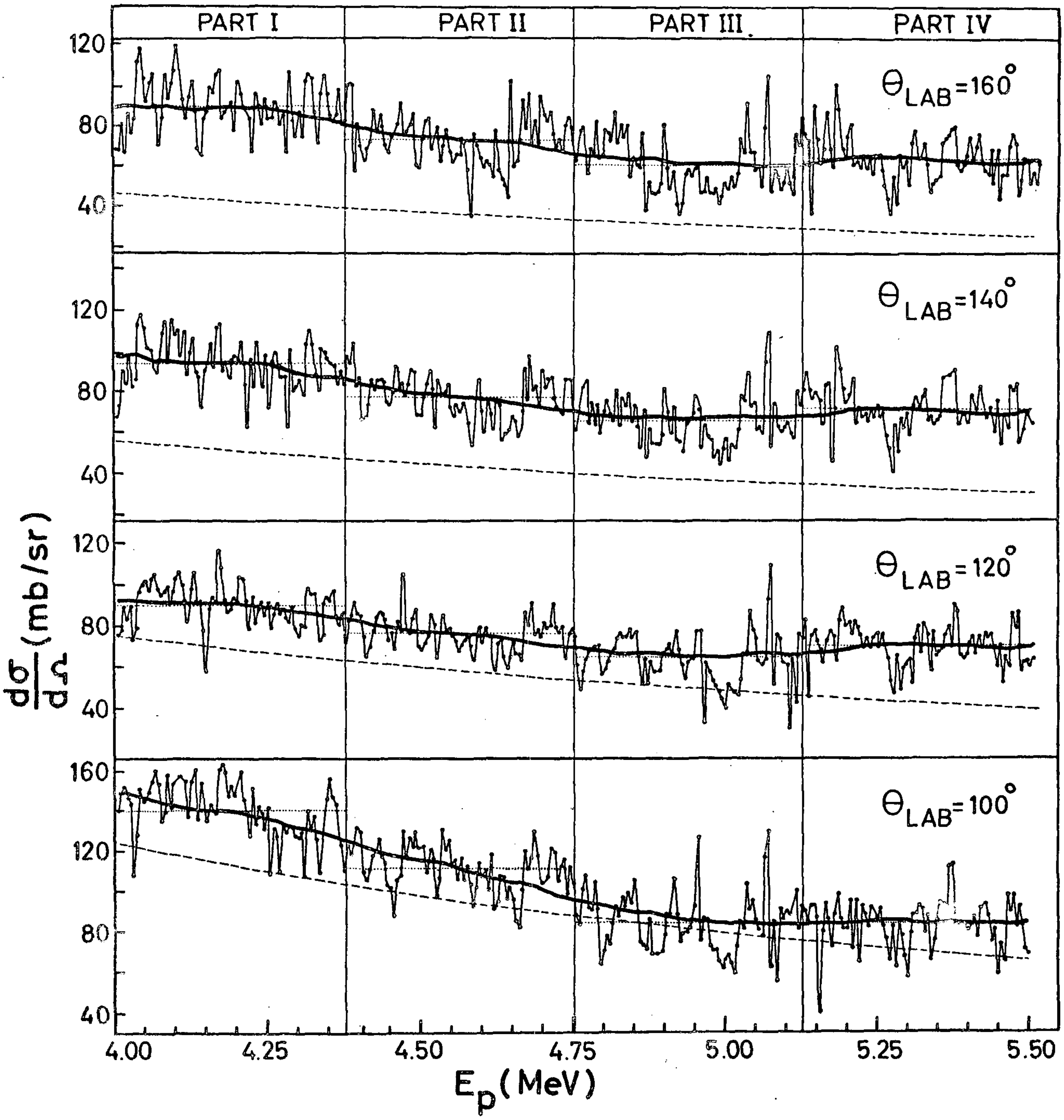

PART I
PART II
PART III
PART IV
$\Theta_{LAB}=160°$
$\Theta_{LAB}=140°$
$\Theta_{LAB}=120°$
$\Theta_{LAB}=100°$
$\frac{d\sigma}{d\Omega}$ (mb/sr)
E_p (MeV)
4.00
4.25
4.50
4.75
5.00
5.25
5.50
40
80
120
160

FIG. 9

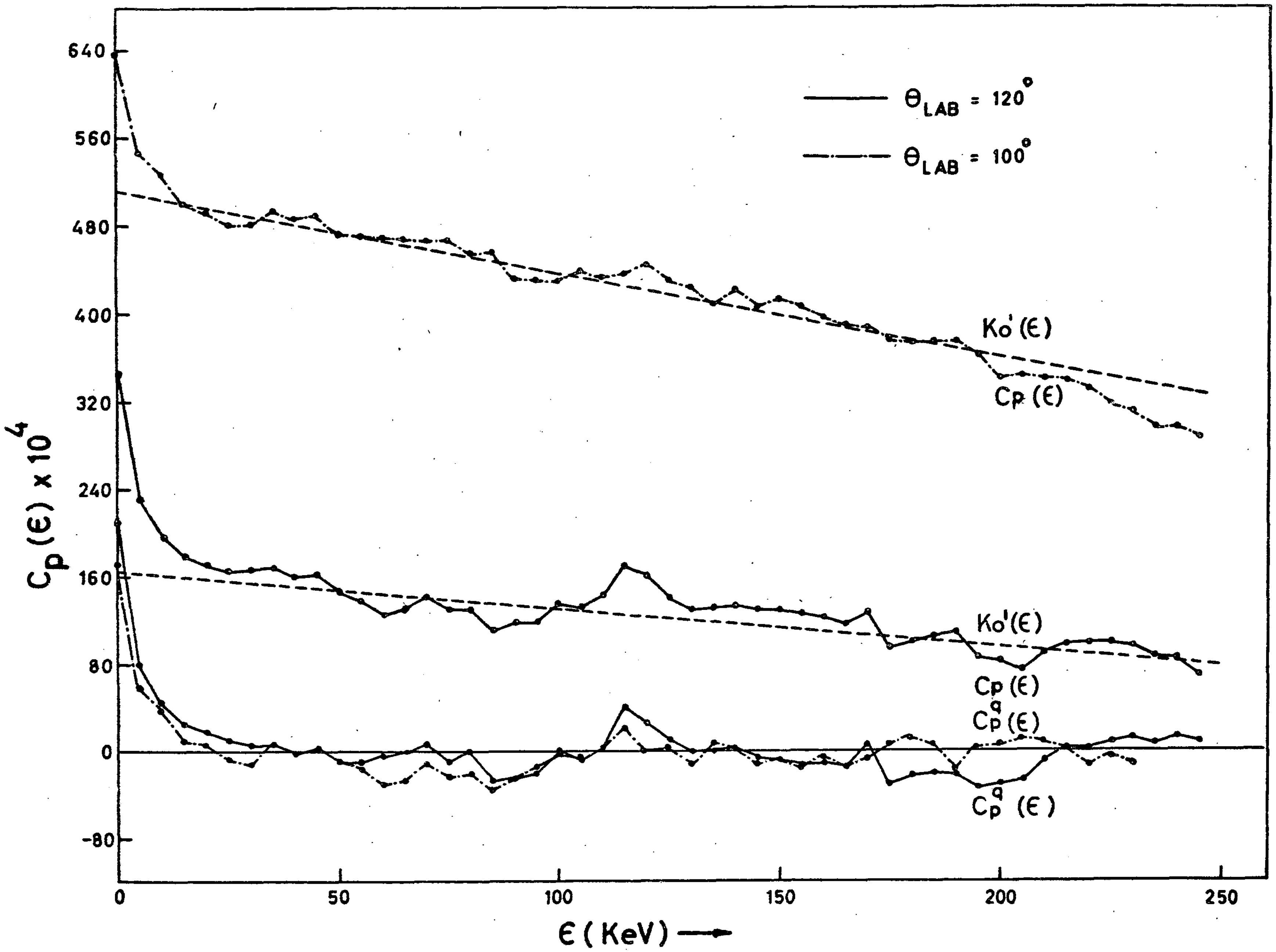

$\Theta_{LAB} = 120°$
$\Theta_{LAB} = 100°$
640
560
480
400
320
240
160
80
0
-80
$C_p(\epsilon) \times 10^4$
$Ko'(\epsilon)$
$Cp(\epsilon)$
$Ko'(\epsilon)$
$Cp(\epsilon)$
$C_p^q(\epsilon)$
$C_p^q(\epsilon)$
0
50
100
150
200
250
ϵ (KeV) →

FIG. 10

TABLE I

θ_{LAB} DEGREES	$C_p(0)$	$K_o'(0)$	$C_p(0)-K_o'(0)$	$C_p^q(0)$	$\Delta C_p(0)$	Γ_{RAW} (KeV)	Γ_{CORR} (KeV)	Γ_q (KeV)	Γ_{CORTI} (KeV)	$\frac{\Delta\Gamma}{\Gamma}$
100	0.0636	0.0512	0.0124	0.0166	±0.0040	22.4	3.5	4.0	3.6	±0.084
120	0.0348	0.0164	0.0184	0.0206	±0.0048	17.3	3.5	4.4	4.0	±0.084
140	0.0422	0.0222	0.0200	0.0236	±0.0048	34.5	4.0	4.1	4.3	±0.084
160	0.0583	0.0300	0.0283	0.0363	±0.0065	24.0	3.5	4.0	4.4	±0.085

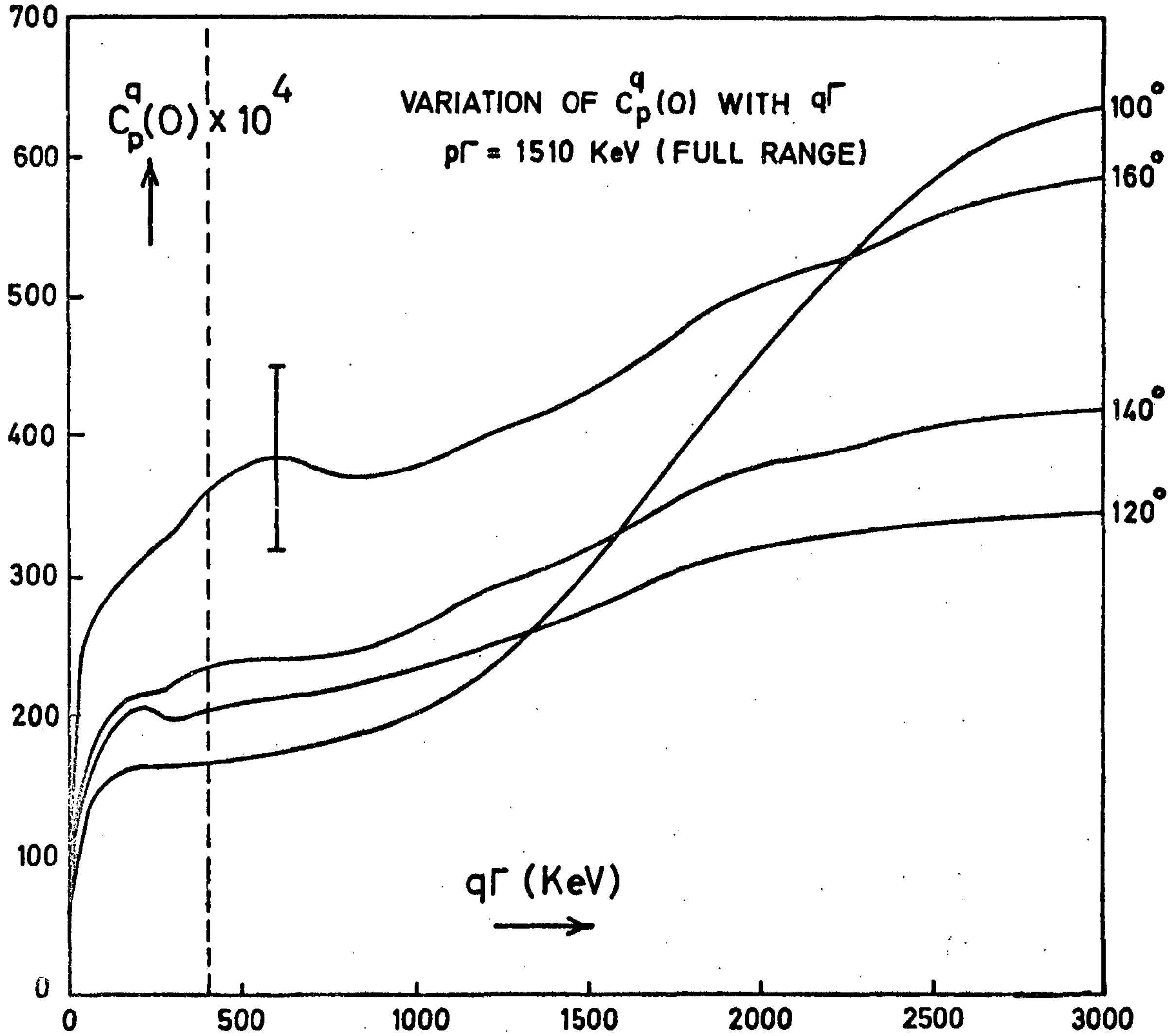

$C_p^q(O) \times 10^4$
VARIATION OF $C_p^q(O)$ WITH $q\Gamma$
$p\Gamma$ = 1510 KeV (FULL RANGE)
$q\Gamma$ (KeV)
100°
160°
140°
120°
0
100
200
300
400
500
600
700
0
500
1000
1500
2000
2500
3000

FIG. 11

function with worse resolution are obtained. If square resolution function, $f_c = \delta E$ new resolutions for the γ^{th} operation is γf_c. In the present case $f_c > \delta E$ so for $\gamma = 1, 2, 3$ ..... excitation function are assumed to have resolution , f_c, $2\delta E$, $3\delta E$, ... respectively.

The function $C_{P}(f)$ is fitted with Gibb's formula[2] for various f values. This function is very sensitive to the value of Γ chosen (Fig.12). The values of Γ obtained are shown in Table I as Γ CORTI.

3.1 Cross correlations: Angular cross correlations were calculated and a rise with increasing $q_i\Gamma$ is found and is ascribed to modulation effects. It is found that cross correlations for (100°, 120°), (100°, 140°), (100°, 160°) are .703, .6076 and .4906 respectively.

Theoretical estimate of coherence angle when y_D is high is difficult to make.

4.1 The energy is then divided in four equal parts (shown by vertical lines in Fig. (9). because firstly y_D is less dependent on energy over a smaller range so that probability distribution analysis to get N and y_D assuming constant y_D is justified and secondly a systematic variation of C(0) and Γ can be studied.

4.2 The auto correlation analysis for 4 parts separately has indicated the following:

(i) As $\sigma_q(E_i)$ do not differ from $\langle\sigma(E_i)\rangle_p$ (dotted lines parallel to energy axis in Fig.(9), $K_0'(0)$ is small and functions and $C_p^q(\epsilon)$ & C_p are identical.

(ii) C(0) varies very much within energy range thus showing variation of γ_D over energy range assuming N constant.

(iii) Γ does not vary with energy within the error of 0.8 KeV.

5.1 Probability distribution: 32 sets of experimentally normalised probability histograms $P_\theta^{E_x}(y)$ for full range and local averages are found quite similar. Theoretical distributions $P_N(y, y_D)$ [3] were also calculated. As N is quite large increase in either N or y_D produces similar effects. As a result large number of (N, y_D) sets fit experimental distributions equally well. These sets (Cf.Fig.13) were restricted by following constraints.

(a) N does not vary through an energy block

(b) $\sigma_D \geq \langle \sigma_{Rulk} \rangle$

(c) such (N, y_D) sets should give a C(0) value which agrees to experimental one within errors (Fig. 13)

Angle	N	y_D			
		Part (1)	Part (2)	Part (3)	Part (4)
100°	24 ± 3	0.85 ± 0.05	0.85 ± 0.05	0.60 ± 0.10	0.70 ± 0.10
120°	20 ± 3	0.83 ± 0.03	0.87 ± 0.05	0.50 ± 0.10	0.75 ± 0.05
140°	20 ± 3	0.80 ± 0.07	0.75 ± 0.05	0.60 ± 0.12	0.70 ± 0.07
160°	15 ± 3	0.76 ± 0.04	0.67 ± 0.05	0.53 ± 0.08	0.67 ± 0.06

As expected by theory N falls at backward angles. Theoretical value of N at 90° is 128 in this present reaction. This prediction of theory is not at all satisfactory as from data $N\ exp = \frac{1}{C_p^{\gamma}(0)}$ at 100° is 60 and any direct process y_D will lower N exp further.

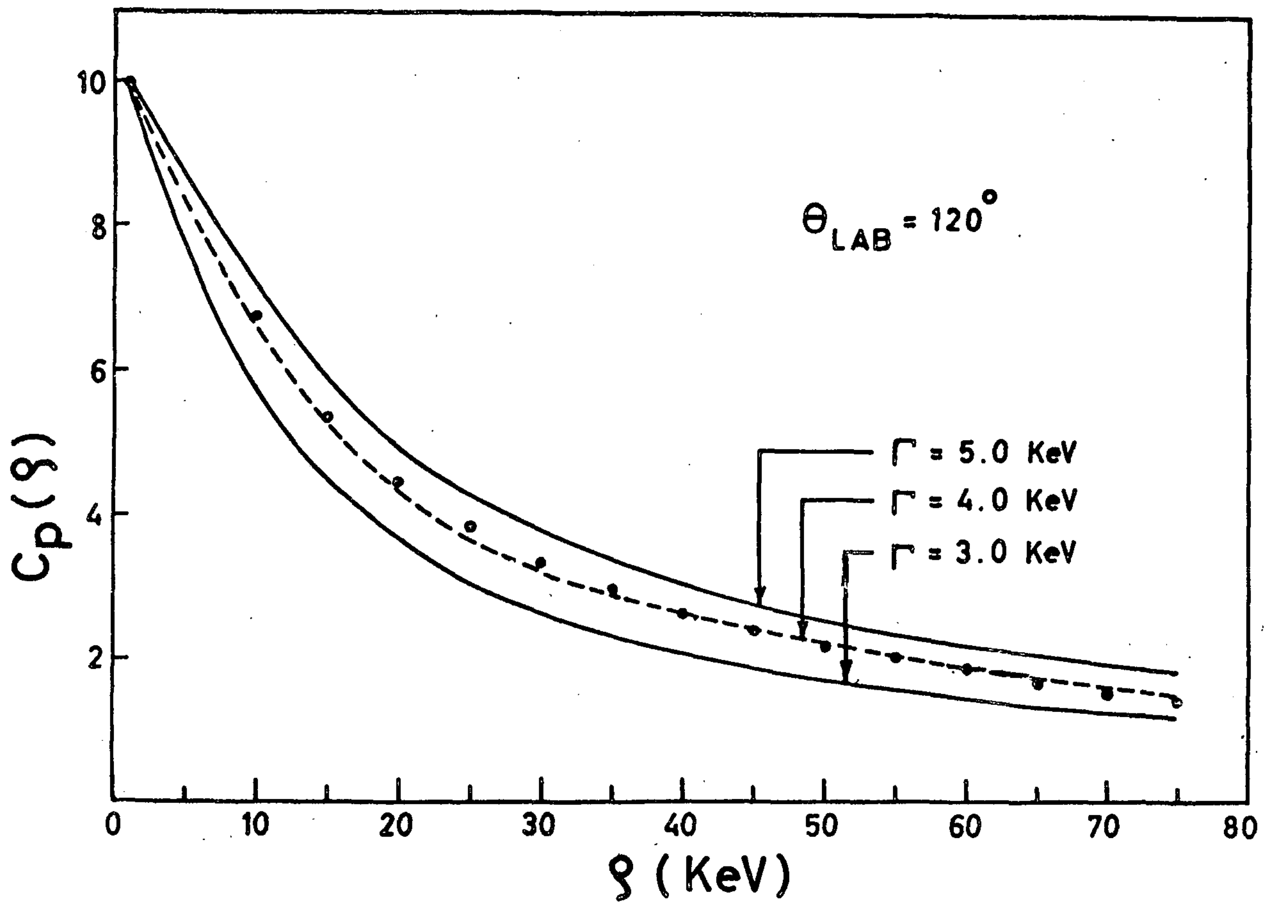
$\Theta_{LAB} = 120°$
$\Gamma = 5.0$ KeV
$\Gamma = 4.0$ KeV
$\Gamma = 3.0$ KeV
$C_p(\varrho)$
ϱ (KeV)
0
2
4
6
8
10
10
20
30
40
50
60
70
80

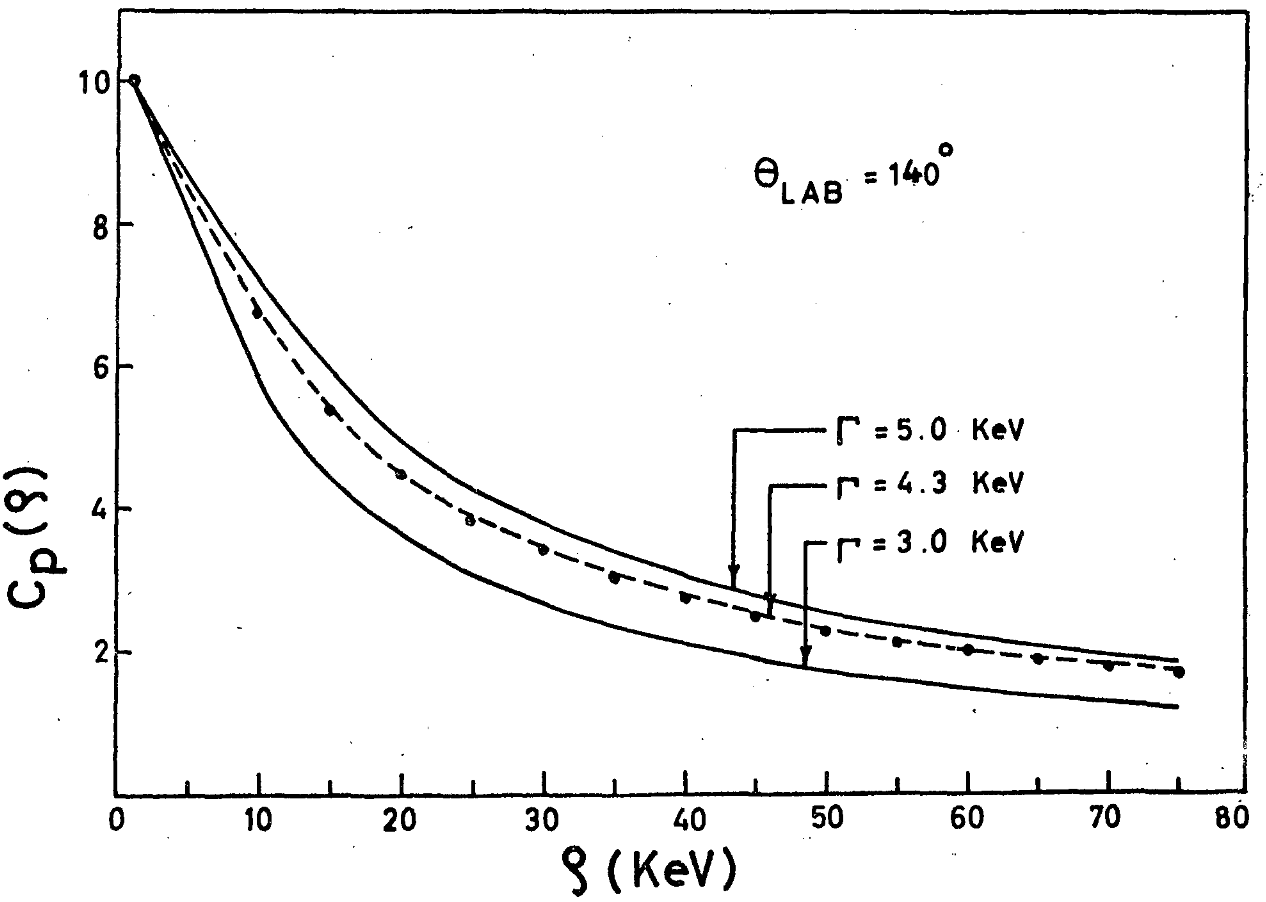
$\Theta_{LAB} = 140°$
$\Gamma = 5.0$ KeV
$\Gamma = 4.3$ KeV
$\Gamma = 3.0$ KeV
$C_p(\varrho)$
ϱ (KeV)
0
2
4
6
8
10
10
20
30
40
50
60
70
80

FIG. 12

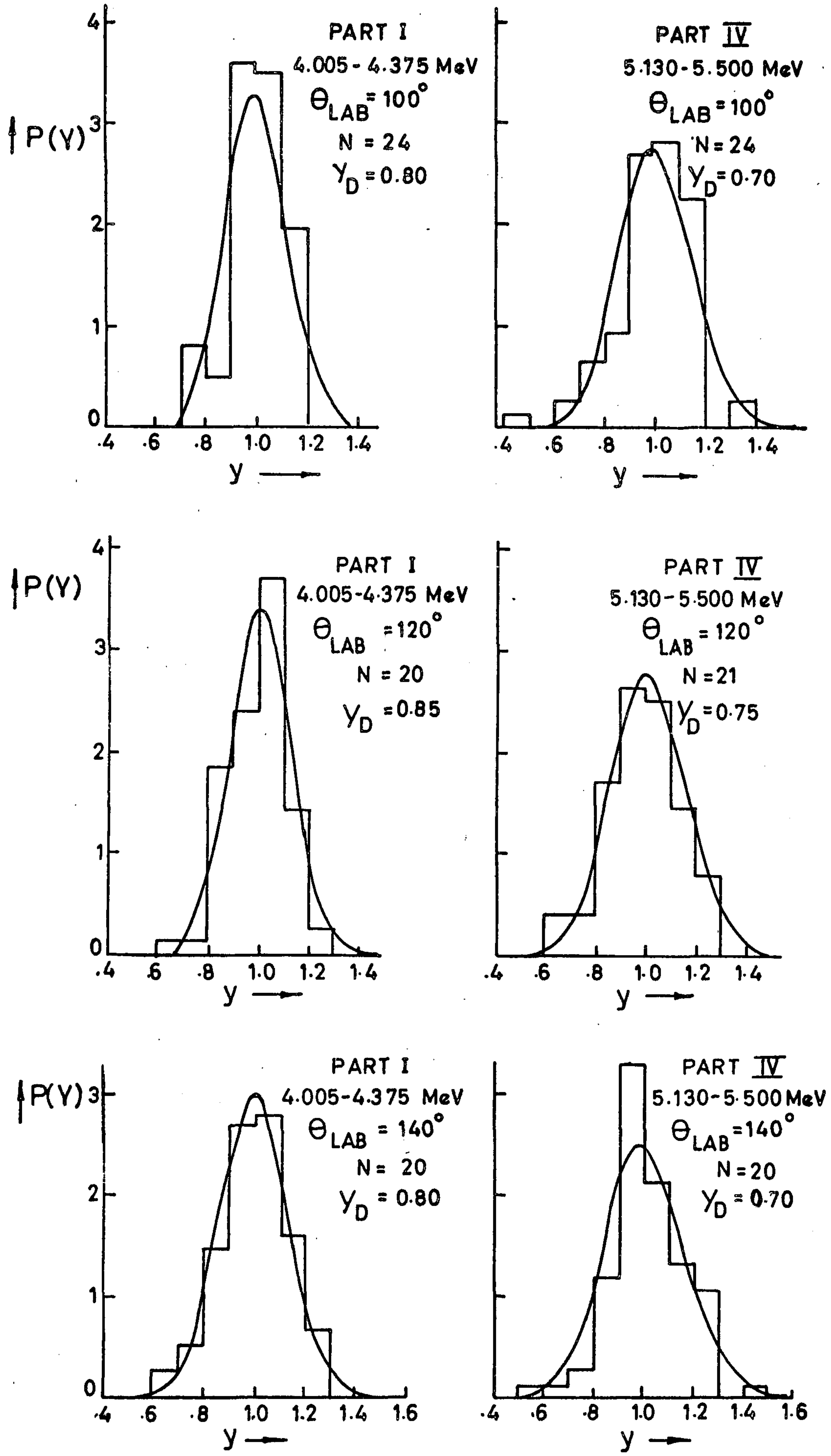

PART I
4.005 - 4.375 MeV
Θ_{LAB} = 100°
N = 24
Y_D = 0.80
PART IV
5.130 - 5.500 MeV
Θ_{LAB} = 100°
N = 24
Y_D = 0.70
PART I
4.005-4.375 MeV
Θ_{LAB} = 120°
N = 20
Y_D = 0.85
PART IV
5.130 - 5.500 MeV
Θ_{LAB} = 120°
N = 21
Y_D = 0.75
PART I
4.005-4.375 MeV
Θ_{LAB} = 140°
N = 20
Y_D = 0.80
PART IV
5.130-5.500 MeV
Θ_{LAB} = 140°
N = 20
Y_D = 0.70
P(Y)
y

FIG. 13

Conclusions:

(1) A large range (energy and angle) of data must be studied so that modulation, which standard theory does not describe, may become apparent.

(2) Γ obtained by different methods agree well but Corti's method is found to be more reliable in present circumstances.

(3) For local averages proper averaging interval should be chosen.

(4) Probability distribution analysis shows that is meaningful to distinguish direct and compound contribution even at high excitations where compound nucleus lives for a very small time.

(5) Probability histograms and normalised variance are unaffected by step size provided sample is large enough.

1) B.W. Allardyce et al. Nucl. Phys. 85 (1966) 193

2) M. Corti et al. Energia Nucleare 13 (1966) 312.

3) Experimental evidence of statistical fluctuations.
T. Mayer Kuckuk. Hercegnovi Lectures.

7. A search for the level at 803 KeV in ^{51}Cr - K.V.K. Iyengar*, B. Lal*, S.K. Gupta* and M.D. Deshpande* - The 803 KeV level found in ^{51}Cr through the $^{50}Cr(d,p)^{51}Cr$ reaction does not seem to be generated in the $^{51}V(p,n)^{51}Cr$ reaction to an intensity greater than 2% of the 747 KeV level as determined by observing the direct gamma radiations with a lithium-drifted germanium detector with incident protons of energy in the range 2.310 - 3.100 MeV.

Published in Nuclear Physics A 93 (1967) 257.

---

* Tata Institute of Fundamental Research, Bombay,

8. Study of the $^{51}V(p,n)^{51}Cr$ reaction - K.V.K. Iyengar*, S.K. Gupta* and B. Lal* - The excitation functions of the 0.75, 1.27, 1.35 and the unresolved 1.50 plus 1.56 MeV gamma rays resulting from the $^{51}V(p,n)^{51}Cr^*$ reaction have been measured from their respective thresholds upto 5.5 MeV. They all vary smoothly with proton energy and exhibit no significant structure. The ratio of the measured yield of the 0.75 MeV gamma rays to that of the 1.17 MeV gamma rays as a function of incident proton energy is compared with the ratio predicted by the Hauser-Feshbach Theory, and the spin of the levels was deduced to be 3/2 and 5/2 respectively. The n_1 - 0.75 MeV gamma and n_2 - 1.17 MeV gamma angular correlations have been measured at proton energies 3.1, 3.3 and 3.5 MeV in the plane of the reaction and at 3.1 and 3.3 MeV in the plane perpendicular to it. The shapes of the measured correlations are not in complete agreement with the predictions of the compound nucleus statistical model and seem to indicate either the preponderance of a cluster of compound nucleus levels or some interference effect.

Published in Nucl. Phys. A 96 (1967) 417.

9. Fluctuations in the integrated cross section of the reaction $^{45}Sc(p,n)^{45}Ti$ - K.V.K. Iyengar*, S.K. Gupta*, K.K. Sekharan, M.K. Mehta and A.S. Divatia - The integrated cross section of the reaction $^{45}Sc(p,n)^{45}Ti$ as a function of incident proton energy has been measured in the energy interval 2.410 to 5.250 MeV with energy steps of 5 KeV. The overall energy

---

* Tata Institute of Fundamental Research, Bombay.

resolution was about 3.5 KeV. The excitation function shows fluctuations around an average. This average increases with proton energy. The statistical theory of Ericson was applied; the auto-correlation was calculated and used to determine the average width of levels in the compound nucleus ^{46}Ti in the excitation energy range 13.230 to 15.140 MeV. The analysis yields an average width $\langle \Gamma \rangle$ of 6 KeV corresponding to a compound nucleus lifetime of 1.1×10^{-19} sec.

Published in Nuclear Physics A 96 (1967) 521.

10. Search for the 0.510 and 0.680 MeV levels in ^{55}Fe and the angular distribution of gamma rays from $^{55}Mn(p,n\gamma)^{55}Fe$ reaction - K.V.K. Iyengar*, B. Lal* and S.K. Gupta* - The 0.510 and 0.680 MeV levels in ^{55}Fe do not seem to be generated in the $^{55}Mn(p,n)^{55}Fe$ reaction to an intensity higher than 5% of the 0.410 MeV level as determined by observing the direct gamma radiations with a lithium drifted germanium detector, with incident protons of energy 2.40 - 3.50 MeV. The measured angular distributions of the 0.933 and 1.322 MeV gamma rays at $E_p = 2.40$ and 3.50 MeV and that of the 1.413 MeV gamma rays at $E_p = 3.50$ MeV are in reasonable agreement with those calculated from statistical model. The reaction proceeds through the compound nucleus and the random phase approximation appears to be valid for the compound nucleus of ^{56}Fe at an excitation energy of about 13 MeV.

To be published in the Proceedings of Nuclear Physics and Solid State Physics Symposium, India (1967).

---

* Tata Institute of Fundamental Research, Bombay.

11. <u>Calculated efficiencies of cylindrical type Ge(Li) detectors</u> - K.V.K. Iyengar* and B. Lal* - Gamma ray detection efficiencies of Ge(Li) detectors of cylindrical shape for point sources placed on the axis of the detector were calculated on a CDC - 3600 computer. Detectors of cross sectional area 1 - 10 sq. cm., depletion depths 2-10 mm and source to crystal distances 1 - 25 cm were chosen for calculation. These efficiencies will be useful for quantitative measurements of gamma-ray intensities in nuclear reactions as well as in the study of the decay of radioactive nuclei.

The detection efficiency ε defined as the ratio of the number of counts to the number of gamma rays emitted by the source is given by the expression

$$\varepsilon = \frac{1}{4\pi}\int\left\{1 - \exp(-\mu x)\right\} d\Omega$$

where x is the thickness of the detector as seen by the gamma ray, $d\Omega$ the solid angle subtended at the source by the detector and μ the total absorption coefficient i.e., the sum of the photoelectric absorption coefficient, pair production absorption coefficient plus the compton absorption and compton incoherent scatter components.

$$x(\theta) = t \sec\theta \quad \text{for} \quad 0 \leq \theta \leq \tan^{-1}\frac{r}{h+t} = \alpha$$

$$x(\theta) = r \operatorname{cosec}\theta - h \sec\theta \quad \text{for} \quad \alpha \leq \theta \leq \tan^{-1}\frac{r}{h} = \beta$$

$$d\Omega = 2\pi \sin\theta \, d\theta$$

The expression for the efficiency was written as the sum of the three integrals

---

* Tata Institute of Fundamental Research, Bombay.

$$\varepsilon = \frac{1}{2}\left[\int_0^{\beta} \sin\theta \, d\theta - \int_0^{2} \exp(-\mu x(\theta)) \sin\theta \, d\theta - \int_0^{\beta} \exp(-\mu x(\theta)) \sin\theta \, d\theta\right]$$

he latter two of which were evaluated using Gauss quadrature method by means of a programme written for CDC - 3600 computer at Tata Institute of Fundamental Research.

Shown in fig.14 is the geometry of the cylindrical detector and fig.15 a family of curves representing the type of total efficiency curves (obtained by calculation) for a Ge(Li) detector of area 2 sq.cm and of depletion depth 2 mm for source heights (measured from the front face of the detector) ranging from 1-25cm.

A programme is also being written for CDC - 3600 computer to calculate the full energy peak efficiencies of cylindrical type Ge(Li) detectors by a Monte Carlo method to take into account multiple interactions of gamma rays in the detector volume to supplement the total efficiency data to make them more useful.

12. <u>Computer programme for calculating (N,N'Y) correlation in nuclear reactions, nucleon angular distributions and gamma angular distributions proceeding through the compound nucleus reaction mechanism</u> - K.V.K. Iyengar* - Satchler and Sheldon have derived expressions for (i) (N,N'γ) angular correlations where N is any nucleon (ii) nucleon angular distributions and (iii) gamma ray angular distributions for cases in which the nuclear reaction proceeds through the compound nucleus reaction mechanism.

---

* Tata Institute of Fundamental Research, Bombay.

The following expressions are valid when there is no intervening unobserved radiation. See references [1-3] for an explanation of the notation used here.

$$W(\theta_1,\theta_2,\varphi) = \frac{\chi^2}{32\pi}\frac{(\hat{J}_2)^2}{(\hat{J}_0)^2}\sum_{\mu,\nu,\lambda,J_1,j_1^{(\pm)},j_2^{(\pm)}}(-)^{J_0-J_1-J_2+J_3+j_2^{(\pm)}}$$

$$\times(\hat{J}_1)^4(\hat{j}_1^{(\pm)})^2(\hat{j}_2^{(\pm)})^2\,\delta_\pm\Big[\langle\mu 0|j_1^{(\pm)}j_1^{(\pm)}\tfrac{1}{2}-\tfrac{1}{2}\rangle$$

$$\times\langle\nu 0|j_2^{(\pm)}j_2^{(\pm)}\tfrac{1}{2}-\tfrac{1}{2}\rangle\Big]\Big[W(J_1J_1j_1^{(\pm)}j_1^{(\pm)};\mu J_0)\Big]$$

$$\times\Big[(\hat{L})^2\langle\lambda 0|LL1-1\rangle W(J_2J_2LL;\lambda J_3)$$

$$+2\Delta\hat{L}\hat{L}'\langle\lambda 0|LL'1-1\rangle W(J_2J_2LL';\lambda J_3)$$

$$+\Delta^2(\hat{L}')^2\langle\lambda 0|LL'1-1\rangle W(J_2J_2L'L';\lambda J_3)\Big]$$

$$\times(1+\Delta^2)^{-1}X(J_1J_1\mu;j_2^{(\pm)}j_2^{(\pm)}\nu;J_2J_2\lambda)$$

$$\times\tau\times S_{\mu\nu\lambda}(\theta_1,\theta_2,\phi) \qquad \text{------(1)}$$

$$\left(\frac{d\sigma}{d\Omega}\right)_N = \frac{1}{8}\chi^2\sum(-)^{J_0-2J_1+J_2-1}(\hat{J}_1)^4(\hat{j}_1^{(\pm)})^2(\hat{j}_2^{(\pm)})^2/(\hat{J}_0)^2$$

$$\times\langle\nu 0|j_1^{(\pm)}j_1^{(\pm)}\tfrac{1}{2}-\tfrac{1}{2}\rangle\langle\nu 0|j_2^{(\pm)}j_2^{(\pm)}\tfrac{1}{2}-\tfrac{1}{2}\rangle$$

$$\times W(J_1J_1j_1^{(\pm)}j_1^{(\pm)};\nu J_0)W(J_1J_1j_2^{(\pm)}j_2^{(\pm)};\nu J_2)\,\tau\,P_\nu(\cos\theta_1) \qquad \text{----(2)}$$

$$\left(\frac{d\sigma}{d\Omega}\right)_\gamma = \frac{1}{8}\chi^2\sum(-)^{J_0+j_2^{(\pm)}-2J_1-2J_2-1.5+J_3}\frac{(\hat{J}_1)^4(\hat{J}_2)^2(\hat{j}_1^{(\pm)})^2}{(\hat{J}_0)^2}$$

$$\times\langle\lambda 0|j_1^{(\pm)}j_1^{(\pm)}\tfrac{1}{2}-\tfrac{1}{2}\rangle W(j_1^{(\pm)}j_1^{(\pm)}J_1J_1;\lambda J_0)W(J_1J_1J_2J_2;\lambda j_2^{(\pm)})$$

$$\times\tau P_\lambda(\cos\theta_2)(1+\Delta^2)^{-1}\Big[(\hat{L})^2\langle\lambda 0|LL1-1\rangle W(LLJ_2J_2;\lambda J_3)$$

$$+(\hat{L}\hat{L}')\langle\lambda 0|LL'1-1\rangle W(LL'J_2J_2;\lambda J_3)$$

$$+(\hat{L}')^2\langle\lambda 0|L'L'1-1\rangle W(L'L'J_2J_2;\lambda J_3) \qquad \text{----(3)}$$

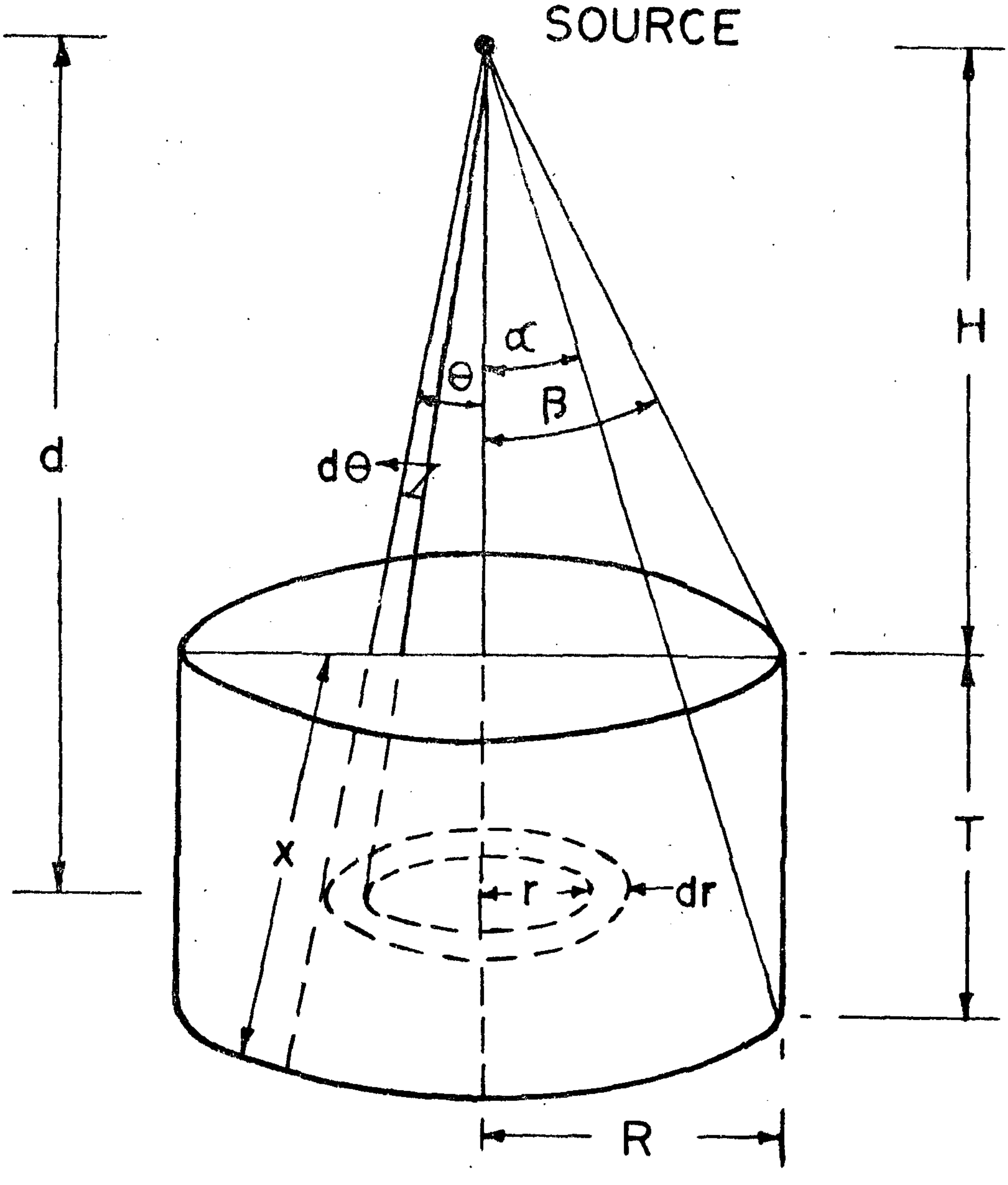

FIG-14

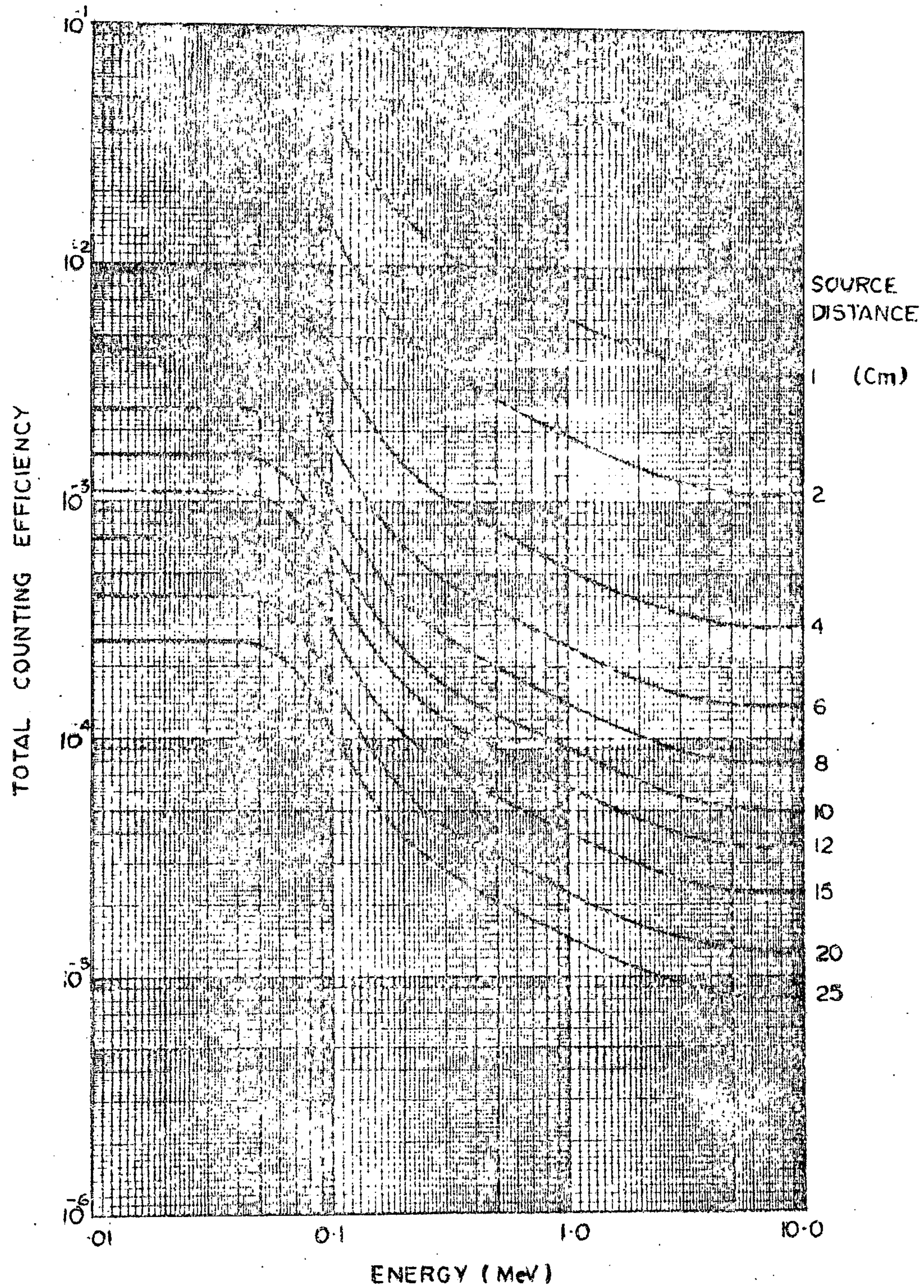

TOTAL COUNTING EFFICIENCY
10^{-1}
10^{-2}
10^{-3}
10^{-4}
10^{-5}
10^{-6}
SOURCE DISTANCE
1 (Cm)
2
4
6
8
10
12
15
20
25
·01
0·1
1·0
10·0
ENERGY (MeV)

FIG-15

Programme in Fortran language have been written for the CDC - 3600 computer at the Tata Institute of Fundamental Research to evaluate the above expressions to obtain nucleon-γ triple correlation and also nucleon and gamma angular distributions. All the three programmes were designed to handle arbitrarily high values of nuclear spin (integer and half integer) and gamma radiation of mixed multipolarity. Results could automatically be obtained not only for a specified multipole mixture (using Δ from input data) but also for $\Delta = 0$ contributions from any number of partial waves could be taken into account in both the incident and exit channels. The programme was capable of taking into account the decay of the compound nucleus through all the energetically allowed channels. The spins and parities of the ground state of the target and residual nucleus and the excited states of the residual nucleus were supplied as inputs. The Q values for excitation of the different states of the residual nucleus (or nuclei when more than one reaction was possible) was also read into the programme as input. A subroutine was used to derive the transmission coefficients at the desired incident and emitted nucleon energies, from the transmission coefficients read into the programme for the incident and emitted nucleons at certain discrete energies for each partial wave. The Clebsch-Gordon coefficients, Racah coefficients, Fano or X coefficients, associated Legendre polynomials and Legendre polynomials which were required in the main expression were evaluated as separate functions as part of the main programme. Typical time taken for evaluating a triple correlation was generally of the order of about 90 secs. The time required for computing nucleon and gamma angular distributions was very much less. These programmes have been extensively used to calculate n_1 - 0.75 MeV gamma ray and n_2 - 1.17 MeV gamma ray angular correlations in $^{51}V(p,n\gamma)^{51}Cr$ reaction and to calculate gamma ray angular distributions in $^{55}Mn(p,n\gamma)^{55}Fe$ reaction and also to calculate the 0.75 MeV and 1.17 MeV gamma ray gamma ray excitation functions in the reaction $^{51}V(p,n\gamma)^{51}Cr$.

1) E. Sheldon, Revs. Mod. Phys. 35 (1963) 795.

2) E. Sheldon, Phys. Rev. 133 (1964) B732.

3) E. Sheldon and D.M. Van Patter, Revs. Mod. Phys. 38 (1966) 143.

13. Kinetic energy distribution of fission fragments in the fission of ^{235}U induced by neutrons with energy ranging from Thermal to 2 MeV - D.M. Nadkarni and B.R. Ballal - Measurements[1] of angular distribution of fission fragments have indicated that there is a large pairing gap of about 2.7 MeV in the transition state spectrum of heavy even-even nuclei. On this basis single particle levels in the transition state spectrum of ^{236}U are not expected to be effective until the energy (E_n) of incident neutrons bombarding the ^{235}U target exceeds about 2.1 MeV. With a view to study the possible dependence of the average kinetic energy of fission fragments $\overline{E}_k$ on the collective levels in the transition spectrum, $\overline{E}_k$ has been measured in the fission of ^{235}U induced by neutrons with energies ranging from thermal to 2.1 MeV. The fission chamber consisted of a gridded ionization chamber filled with pure Argon gas at 1.5 atm. The cathode of the ion chamber was coated with 100 $\mu g/cm^2$ ^{235}U.

The cathode-grid and grid-collector distances were 2.1 cms and 0.7 cms respectively. The chamber was operated for optimum performance with cathode, grid and collectors at 0V, + 425 V and + 1050 V respectively and the collector pulse height spectrum was recorded on a 100-channel analyzer after amplification. Neutrons of energy 300 KeV to 2.13 MeV were obtained from $T(p,n)^3He$ reaction using the 5.5 MeV Van de Graaff Accelerator. The tritium target thickness was about 100 KeV for 1 MeV protons. Energy calibration was achieved using thermal neutron induced fission and this was done by surroundimg the chamber with thick paraffin blocks. For the fast neutron runs the energy region from 300 KeV to 2.1 MeV was divided into 21 roughly equal divisions and each one was selected at random. At each of these energies 2.5×10^4 to 7.5×10^4 events were recorded. From the measured spectrum $\bar{E}_k$ was obtained and corrections were made for the motion of the centre of mass[2]. $\left[\bar{E}_k(E_n) - \bar{E}_k \text{ (thermal)}\right]$ versus E_n is shown in Fig.16.

E_k found to remain essentially constant within about 0.6% ($\simeq$ 1 MeV) when the incident neutron energy was varied from thermal to 2.1 MeV. Within this limit however, there is an indication of small dip at $E_n \simeq$ 370 KeV and 870 KeV and a small peak at $E_n \simeq$ 650 KeV and 1.24 MeV. Although some of these variation could be attributed to statistical fluctuation the possibility that these are associated with the nature of the transition states accessible at these energies canmot be ruled out. Blyumkina et al[3] have observed a dip at $E_n \simeq 400$ KeV and a smaller dip around 1 MeV and a peak at $E_n \simeq$ 770 KeV.

The energy balance equation is $Q + E_n = \bar{E}_k + \bar{E}_\nu + \bar{E}_\gamma$ where $\bar{E}_k$ is the average total kinetic energy of the fragments, $\bar{E}_\nu$ and $\bar{E}_\gamma$ are the average energy emitted in the form of prompt neutrons and gamma rays respectively. Assuming that $\bar{E}_\gamma$ is independent of incident neutron energy, as reported by Protopopor et al[4], the variation of the average number of prompt neutrons emitted per fission ($\bar{\nu}$) with E_n have been calculated using the measured values of $\bar{E}_k$ and compared with the measured values of $\bar{\nu}$ (Fig.17). The measured as well as the calculated $\bar{\nu}$ do not show a monotonically increasing dependence of $\bar{\nu}$ on E_n. The calculated values are consistently higher than the measured ones probably due to an increase of $\bar{E}_\gamma$ and of the average energy of the prompt neutrons with increasing E_n. Also the number and average energy of prescission neutrons may vary with E_n. In view of these considerations $\bar{\nu}$ vs E_n data is not very suitable for studying the variation of internal excitation energy of fission fragments with E_n. The most convenient is to look for the variation of E_k with E_n.

Blyumkina et al[3] have suggested that these variation can be accounted for by assigning a higher $\bar{E}_k$ for states having odd spin-parity. However, the observed variation can also come about if there is a rapid variation of the fragment mass distribution with E_n. In particular an increase of symmetric yield results in a decrease of E_k. Cunninghame et al[5] observed a decrease in peak to valley ratio of the mass distribution as E_n is increased from 65 KeV to 1 MeV. It is possible to correlate the dependence of average kinetic energy, excitation energy and

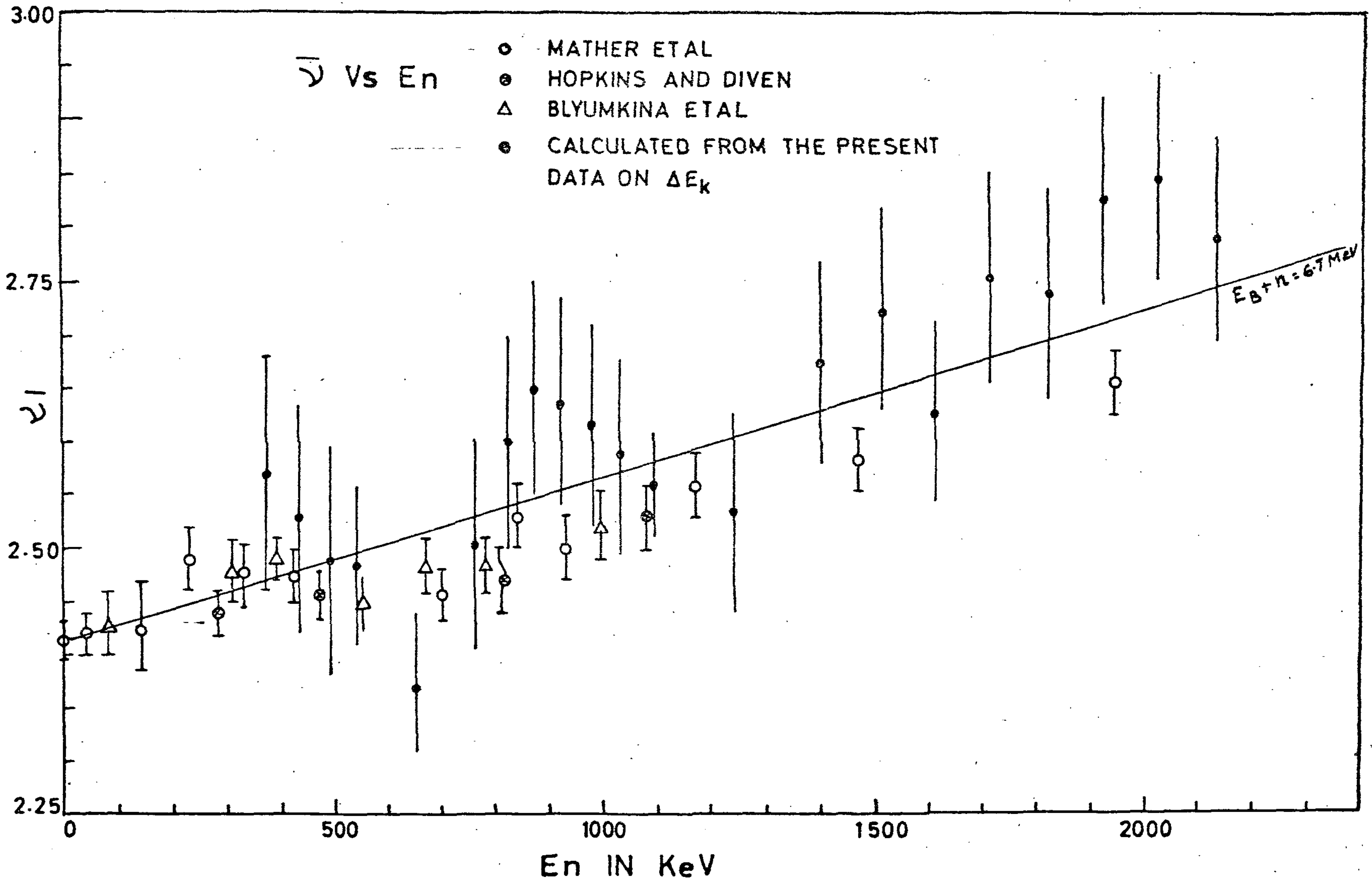

$\bar{\nu}$ Vs En
MATHER ETAL
HOPKINS AND DIVEN
BLYUMKINA ETAL
CALCULATED FROM THE PRESENT DATA ON ΔE_k
$E_B + n = 6.7$ MeV
3.00
2.75
2.50
2.25
$\bar{\nu}$
0
500
1000
1500
2000
En IN KeV

FIG-16

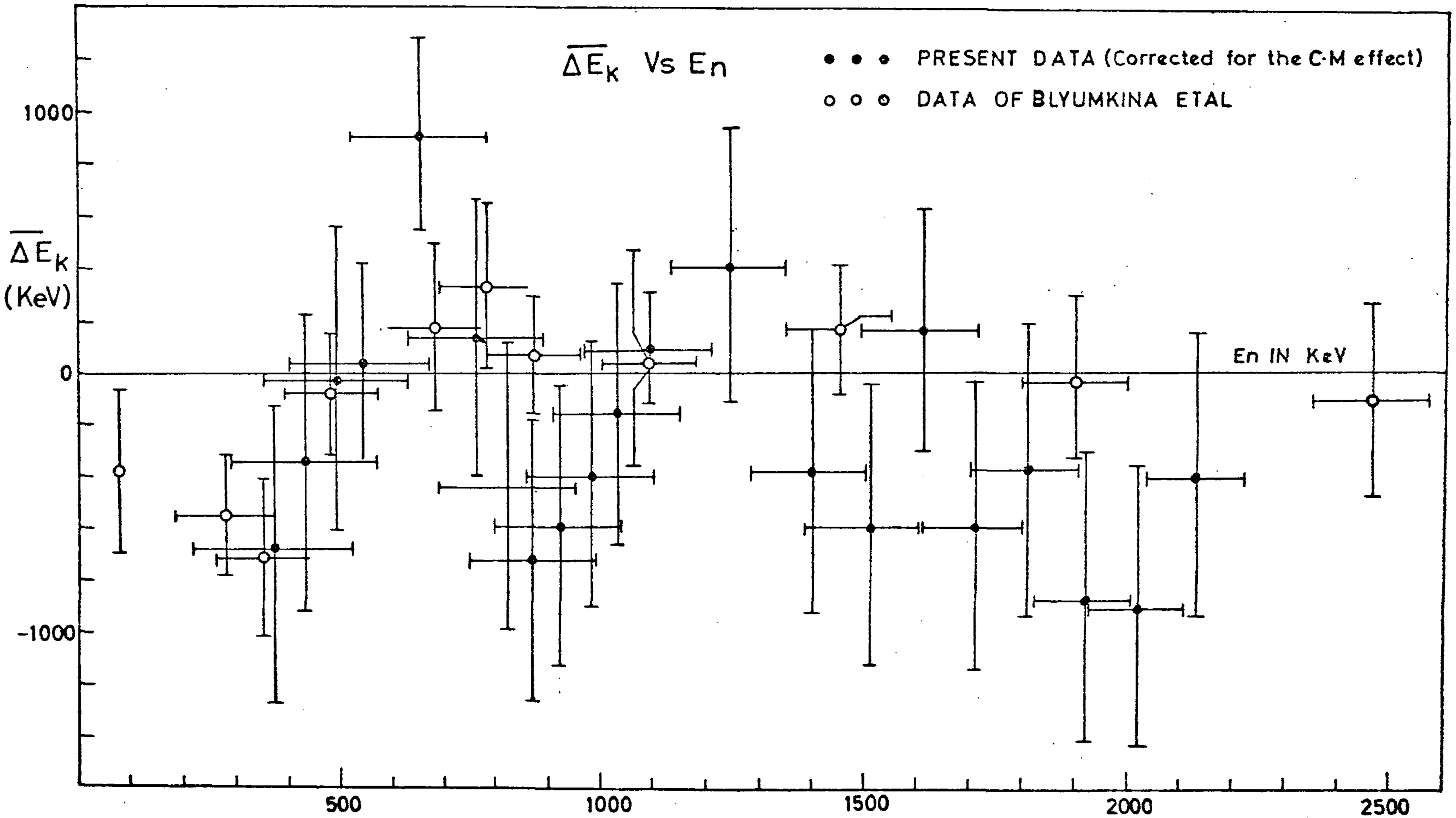

$\overline{\Delta E}_K$ Vs En
PRESENT DATA (Corrected for the C·M effect)
DATA OF BLYUMKINA ETAL
$\overline{\Delta E}_K$ (KeV)
1000
0
-1000
En IN KeV
500
1000
1500
2000
2500

FIG-17

mass distribution on the collective states of the transition state spectrum on the basis of the collective models of Bohr[6] and Wheeler[7].

1) H.C. Britt, et al. Phys. Rev. Letts. 11, (1963) 343.

2) J.S. Wahl, Phys. Rev. 95, (1954) 126.

3) Yu.A. Blyumkina et al. Nucl.Phys. 52, (1964) 648.

4) A.N. Protopopov and B.M. Sirijager, JETP 7,(1958) 231.

5) J.G. Cunninghame et al, Nucl. Phys. 27, (1961) 154.

6) A. Bohr, Proc. Int. Conf. At En. 2, (1956) 911.

7) J.A. Wheeler, Fast Neutron Phys. Part II, (1963).

14. Angular anisotropy of fission fragments in 3 MeV neutron induced binary and ternary fission of ^{235}U - D.M. Nadkarni - To understand the mechanism of ternary fission, fission accompanied by long range alpha particles (LRA), it is important to know at what stage of the process these particles are emitted. The measurement of fragment angular distributions in ternary fission can be expected to provide an understanding about the stage at which LRA are emitted. Previous measurements[1] of anular distribution fragments in ternary fission indicated that the anisotropies in binary and ternary fission are different. In the present work using solid state detectors the anisotropy of fragments in ternary fission of U^{235} induced by 3 MeV neutrons has been measured.

Two diffused-junction type solid state detectors were used to detect fission fragments emitted along and at right angles to the incident neutron beam direction and the third solid state detector was kept very close to the fissile target to detect LRA in nearly 2π geometry, (Fig. 18). ^{235}U target was 1 mg/cm^2 thick on a 3 mg/cm^2 Al backing which allowed only LRA to reach the back detector. 3 MeV neutrons were produced with $T(p,n)^3He$ reaction using the 5.5 MeV Van de Graaff Accelerator. The very low cross-section for fast neutron induced ternary fission necessitated keeping the fragment detectors near the target resulting in poor angular resolution ($\simeq 35^\circ$). The spectra of fission fragment kinetic energy in 0° -and 90° -detectors in coincidence and anti-coincidence with the LRA pulse were recorded simultaneously in four 100-channel analyzers. Efficiency correction factors for 3 MeV neutron induced binary and ternary fission were made using the isotropic fragment distribution in thermal neutron induced binary and ternary fission respectively. The thermal neutron measurements were carried out by surrounding the fission chamber with paraffin blocks and keeping the chamber configuration constant. About 810 events of 3 MeV neutron induced ternary fission and about 1590 events of thermal neutron induced ternary fission were recorded in a series of runs lasting nearly 100 hours.

The results of these measurements are (i) Binary fragment anisotropy ($N(0^\circ)/N(90^\circ) = 1.04 \pm 0.01$ (ii) Ternary fragment anisotropy ($N(0^\circ)/N(90^\circ) = 0.87 \pm 0.06$ (iii) The ternary to binary cross-section ratio was found to be about 50% and 25% lower for 3 MeV neutron fission as compared to thermal neutron fission in the 0° and 90° directions respectively. (iv) The decrease in the average kinetic energy of ternary fission fragments compared to that of binary fragments was found to be approximately equal (14 ± 3 MeV) both in the thermal and 3 MeV neutron induced

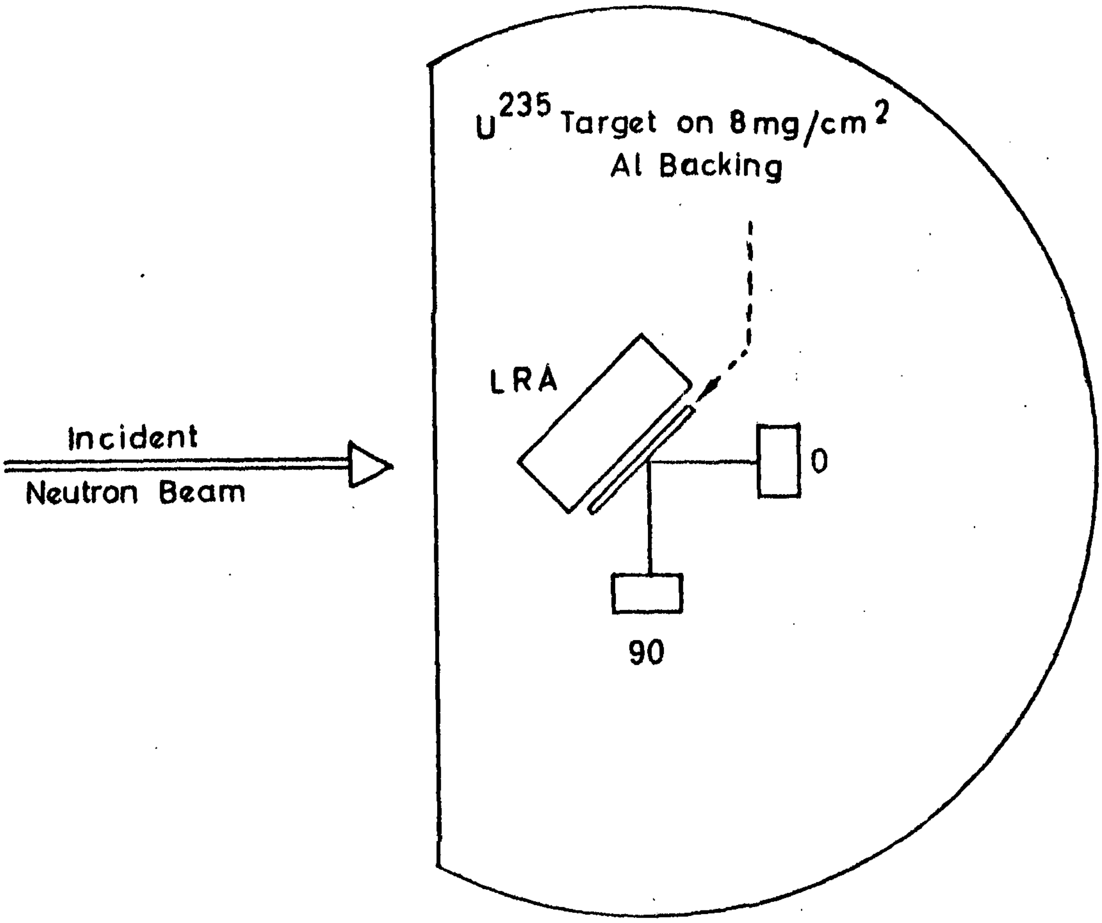
U^{235} Target on 8 mg/cm^2
Al Backing
LRA
Incident
Neutron Beam
0
90

FIG 18

fission.

The rather low binary anisotropy is attributed to the poor angular resolution as well as to the variation of the neutron flux across the fissile target. The binary fragment anisotropy was separately measured for the case where the neutron flux is nearly uniform across the fissile target and was found to be 1.107 ± 0.017. Using the values of binary anisotropies measured in the present work and that reported by Simmons and Henkel[2], approximate correction for the angular resolution and non-uniform flux of neutrons across the target have been made to the ternary fission data. The corrected ternary anisotropy was found to be (0.91 ± 0.07).

It is of interest to correlate (n,α) anisotropy in 3 MeV neutron induced ternary fission of ^{235}U [3] with the anisotropy of ternary fragments measured in the present work. According to the Evaporation Model[1] the angular distribution of LRA is given by

$$n_\alpha(\theta) \simeq 1 + \frac{\alpha^2 \bar{I}^2 \bar{\ell}^2}{2} \cos^2\theta \approx a + b\cos^2\theta$$

Imposing on this the condition that LRA and ternary fission fragments are emitted at right angles to each other, the ternary fragment angular distribution obtained is $n_{tf}(\theta) \simeq a + \frac{b}{2}\sin^2\theta$. Using the LRA anisotropy[3] of 1.32 ± 0.12 this gives for the ternary fragment anisotropy a value of 0.86 ± 0.05 which is in fair agreement with the value obtained in the present measurements. The results of the present work suggest that due to the emission of LRA the K-distribution at the scission state in ternary fission is different from that in binary fission.

1) R.Ramanna, K.G. Nair and S.S. Kapoor, Phys.Rev.129, (1963) 1350; D.M. Nadkarni, Proc.Nucl.Phys.Symposium, India (1966) 35.

2) J.E. Simmons and R.L. Henkel, Phys. Rev.120,(1960) 198.

3) V.A. Hattangadi, T.Methasiri, D.M. Nadkarni, R. Ramanna and P.N. Rama Rao, SM-60/71, IAEA Symposium on Phys & Chem. of Fission, Salzburg (1965).

15. Total and partial widths for levels in ^{17}O - A.S. Divatia, K.K. Sekharan and M.K. Mehta - Total widths for 16 levels in ^{17}O, in the excitation energy region 7.9 to 10.5 MeV have been obtained from a study of the total cross section for the $^{13}C(\alpha,n)^{16}O$ reaction[1], for the incident alpha energy range 1.95 - 5.57 MeV, using a 4π neutron detector. Partial widths Γ_α and Γ_n and the corresponding reduced widths γ_α^2 and γ_n^2 have been determined for the four levels at 8.40, 8.50, 9.19 and9.88 MeV.

To be published in the Physical Review.

1) K.K. Sekharan, A.S. Divatia and M.K. Mehta, Proceedings of N.P. and S.S.P. Symposium, India, (1966) 93.

16. Study of the structure in the excitation functions for the reactions $^{27}Al(p,\alpha_0)^{24}Mg$ and $^{27}Al(p,\alpha_1)^{24}Mg^*$ - M.K. Mehta, A. S. Divatia, S.S. Kerekatte and K.K. Sekharan - In continuation of previous work[1], the yields from the reactions $^{27}Al(p,\alpha_0)^{24}Mg$ and $^{27}Al(p,\alpha_1)^{24}Mg^*$ have been measured at a few angles for the range of proton bombarding energy from 4 to 5.5 MeV. The excitation functions reveal a gross structure on which finer variations are superimposed. A cross-correlation analysis is under progress to determine whether the strong resonance like stfuctures

are indeed resonances representing individual levels in the compound nucleus ^{28}Si and not the so called Ericson fluctuations.

1) M.K. Mehta and A.S. Divatia, Proceedings of the N.P. and S.S.P. Symposium India (1966) 80.

17. <u>A non-linear least square fit programme for gaussian fitting</u> - S.K. Gupta* - A non linear least square fit programme for fitting the pulse height spectra with gaussian peaks and flat background has been written up combining the exact process of linear least square fitting for linearly occuring parameters and minimizing process of a non-linear function. Davidon[1] and Fletcher and Powell[2] process has been used for the latter. It has been observed that this combination speeds up the fitting. The time taken on the CDC - 3600 computer for one peak is ~ 3 seconds. Already 225 spectra of 100 channels each have been analyzed. The form $A \exp(-(n - N_0)^2/\sigma^2)$ seemed better than the form $\frac{A}{\sigma} \exp(-(N - N_0)^2/\sigma^2)$ for gaussian. With first form the process always succeeded but with the second form the process failed $\sim 30\%$ times giving inaccurate estimates of variance - convariance matrix.

1) W.C. Davidon, ANL-5990 (Rev.), 1959.
2) R. Fletcher and M.J. D. Powell, Computer Journal (1963),163.

18. <u>The 6.57 MeV level in ^{10}B</u> - K.B. Nambiar, M.Balakrishnan and M.K. Mehta - The 6.57 MeV energy level in ^{10}B has been studied by the elastic scattering of α-particles from ^{6}Li. This level appears to be well-isolated from the neighbouring ones and it should, therefore, be possible to assign spin and

* Tata Institute of Fundamental Research, Bombay.

parity by the application of the single level resonance theory. However, the channel spin 1 involved in this reaction, makes the job rather complicated.

Selecting four angles which correspond to the zeroes of the Legendre polynomials P_4, P_3, P_4 & P_2, excitations were obtained in the energy range $E_{\alpha}^{(lab.)} = 3.00$ MeV to $E_{\alpha}^{(lab.)} =$ 4.42 MeV in steps of 10 KeV. The spectrometer consisted of four solid state detectors mounted at laboratory angles 43°, 56°, 71° and 84° which correspond to the zeroes of the Legendre polynomials P_4, P_3, P_4 and P_2. The pulses obtained, after suitable amplification were fed into a TMC 400 channel analyzer. A current integrator was used to measure the total charge deposited by the α-beam in a Faraday cup, during each run.

A typical excitation curve obtained at $\theta_{lab.} = 56^{\circ}$ is shown in fig.19. The anomaly observed at $E_{\alpha}(lab.) = 3.50$ MeV exhibits striking changes in the shape at the four angles. This is more obvious in fig.20. A shape analysis of the resonance is being done in order to determine the spin and parity of the corresponding 6.57 MeV level in ^{10}B. A general computer programme for analysing the cross sections of elastically scattered α-particle by shape fitting is being written. This programme makes use of Wigner's R-matrix formalism using single level approximation for a general case of arbitrary spin. If a successful shape analysis can be performed on the resonance at 3.5 MeV, it will be tried on other resonances too.

FIG-19

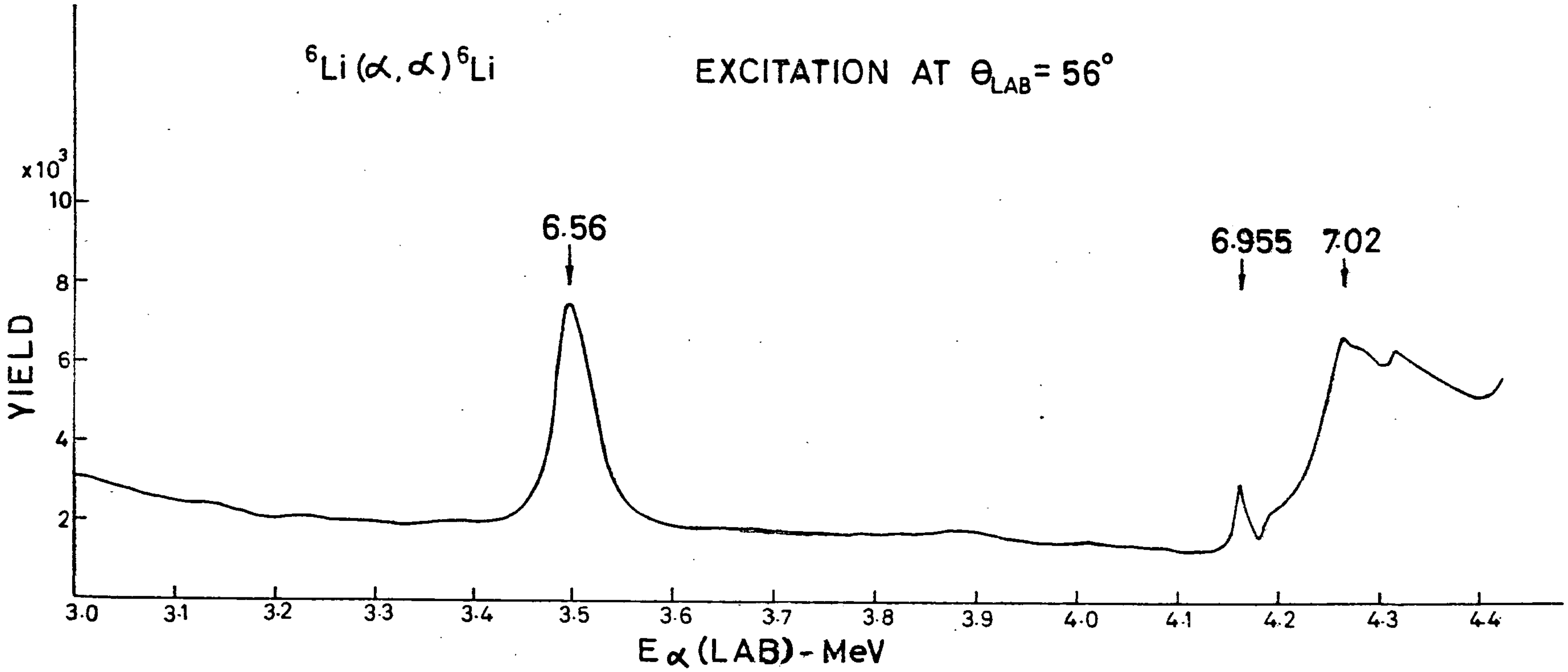

$^6Li(\alpha,\alpha)^6Li$
EXCITATION AT θ_{LAB} = 56°
x10³
10
8
6
4
2
YIELD
6.56
6.955
7.02
3.0
3.1
3.2
3.3
3.4
3.5
3.6
3.7
3.8
3.9
4.0
4.1
4.2
4.3
4.4
Eα (LAB) - MeV

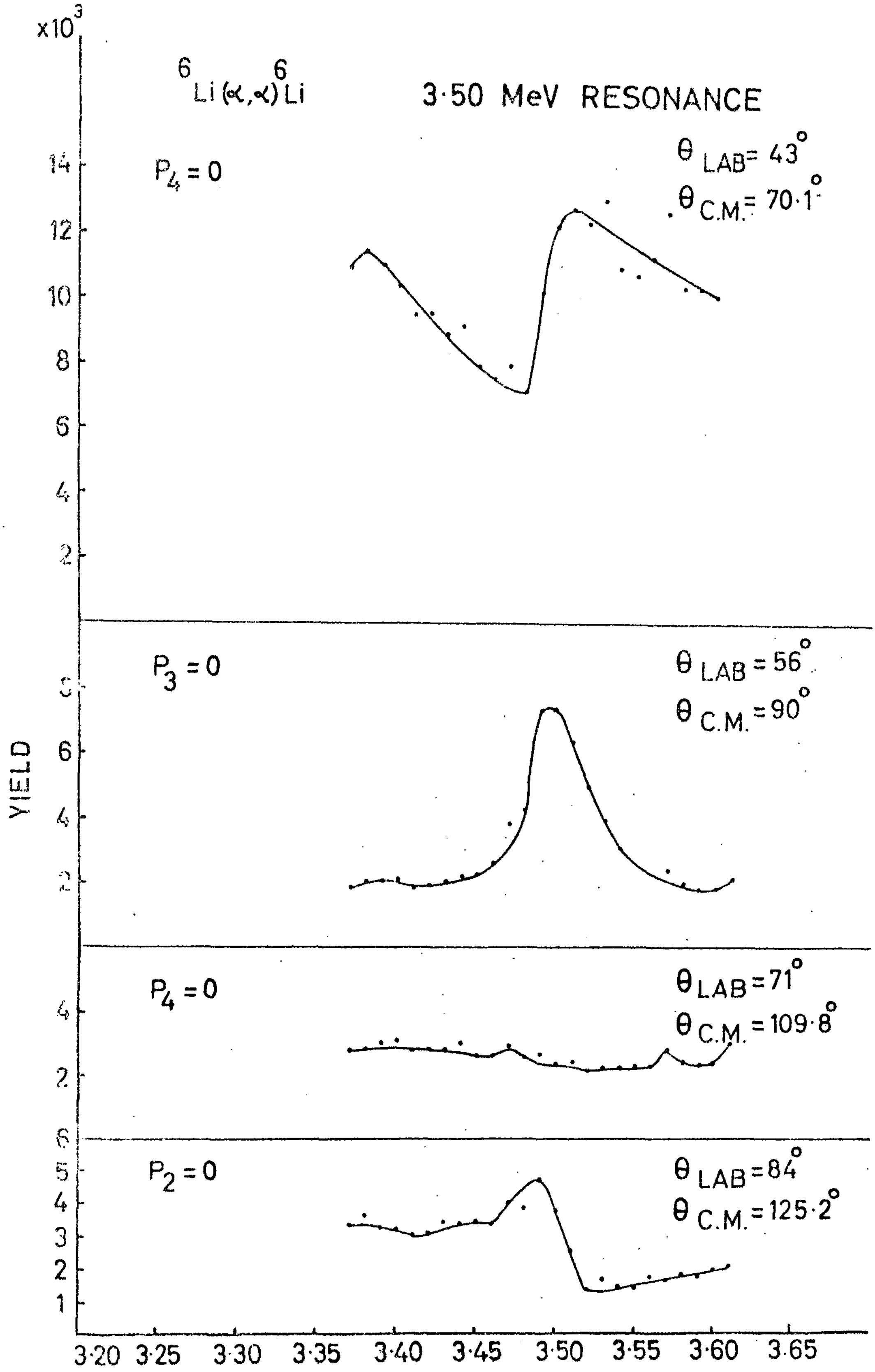

$^{6}Li(\alpha,\alpha)^{6}Li$
3·50 MeV RESONANCE
$\times 10^3$
YIELD
$P_4 = 0$
$\theta_{LAB} = 43°$
$\theta_{C.M.} = 70·1°$
$P_3 = 0$
$\theta_{LAB} = 56°$
$\theta_{C.M.} = 90°$
$P_4 = 0$
$\theta_{LAB} = 71°$
$\theta_{C.M.} = 109·8°$
$P_2 = 0$
$\theta_{LAB} = 84°$
$\theta_{C.M.} = 125·2°$
3·20 3·25 3·30 3·35 3·40 3·45 3·50 3·55 3·60 3·65
E_α - MeV (LAB)

FIG-20

19. Study of the energy levels of odd mass isotopes of In, Ag, Rh and Nb by the inelastic scattering of protons - V.R. Pandharipande*, K.G. Prasad* and R.P. Sharma* - The energy levels of the odd mass isotopes of In, Ag, Rh and Nb have been studied by the inelastic scattering of protons of energy 3.5, 4.0 and 4.5 MeV. The emitted gamma radiation in this reaction has been observed on a lithium drifted germanium detector. The yield of various transitions as a function of energy has been determined. The various excited states in the above-mentioned nuclei have been established by combining the present data with the earlier known energy levels in this region.

20. Coulomb excitation studies in ^{127}I - S.H. Devare*, P. N. Tandon* and H.G. Devare* - The gamma spectra in the Coulomb excitation of ^{127}I have been studied using both a scintillation and a high resolution Ge(Li) solid state detector. Alpha particles and protons accelerated upto 5.25 MeV energy in the Van de Graaff machine were used for these studies. The gamma spectra recorded at various charged particle energies were analyzed and the excitation curves plotted from the thick target yields. The B(E2) values for the excitation of various levels were calculated taking into account the branchings and conversion coefficients known from radioactive decay.

21. On the estimation of background in (X,Gamma) reactions - M.N. Viswesvariah - A method for the determination of the amplitude of the photopeak in a measured gamma spectrum in the

* Tata Institute of Fundamental Research, Bombay.

presence of an unknown background is proposed. This involves a geometrical construction making use of the top of the photopeak, the compton edge and the valley point. It is useful for gamma energies up to 2 MeV. A criterion is also proposed for the determination of the foot of the photopeak from where background subtraction can begin in the study of gamma spectra of radio nuclides. The method is useful for single gamma energies or gamma energies whose photopeaks are separated further apart than the photopeak - compton edge separation for a single gamma energy. The proposed procedure can be adopted for a computer programme in the analysis of gamma spectra.

22. <u>The $^{12}C(^{3}He,p)^{14}N$ and $^{12}C(^{3}He,^{3}He)^{12}C$ reaction</u> - N. S. Thampi, C.M. Lamba, N. Sarma and D.K. Sood* - The angular distributions for the reactions $^{12}C(^{3}He,P)^{14}N$ and $^{12}C(^{3}He,^{3}He)^{12}C$ for various outgoing proton groups have been measured in steps of 10 KeV at an incident energy around 5.3 MeV from the Van de Graaff accelerator. Angular distributions are found to be invariant with energy. These have been fitted with a series of Legendre polynomials. A DWBA analysis of elastic scattering of ^{3}He is being performed to yield optical model parameters which are to be utilised for DWBA analysis of reactions.

* Indian Institute of Technology, Kanpur.

INSTRUMENTATION AND DATA PROCESSING

1. A circuit for preventing accumulation of experimental data when the nuclear reaction rate exceeds a preset value - S.K. Gupta*, K.V.K. Iyengar* and P.J. Bhalerao - A circuit has been devised to restrict accumulation of (n,γ) angular correlation data in $A(x,n\gamma)B$ type reactions only, to periods when the counting rate in the gamma detector is below the fatigue level of the photomultiplier and its gain insensitive to changes in the counting rate.

Published in Nucl. Instr. and Meth. 44 (1966) 123.

2. An anti-coincidence ring counter around Ge(Li) detector - P.J. Bhalerao and K.V.K. Iyengar* - An anti-coincidence ring counter using a 10 cm. thick plastic scintillator of about 30 cm dia. is being developed (since NaI(Tl) scintillators of this size are not available) to anti-coincidence gate the pulses observed in Ge(Li) detector of 1.8 cm diam. and 0.2 mm depletion depth. The light flashes generated in the plastic scintillator by compton scattered gamma rays escaping from the Ge(Li) detector will be collected by a bank of four RCA 6342A photomultipliers, whose anode outputs are connected in parallel. The pulse generated at the anode after suitable amplification will be used to anti-coincidence gate the spectrum in the Ge(Li) detector with the object of reducing the intense compton tail due to high energy gamma rays otherwise present to facilitate detection and measurement of the

---

* Tata Institute of Fundamental Research, Bombay.

intensity of weak low energy gamma rays riding on the compton tail of higher energy gamma rays. It is planned to use this detector assembly by itself and also in conjunction with a large NaI(Tl) crystal and photomultiplier assembly for study of gamma rays from $^{45}Sc(p,n)^{45}Ti$, $^{51}V(p,n)^{51}Cr$, $^{55}Mn(p,n)^{55}Fe$ etc. to obtain information on the decay schemes of the levels of ^{45}Ti, ^{51}Cr, ^{55}Fe etc.

3. <u>Fast discriminator circuits</u> - M.Y. Vaze and K.V.K.Iyengar* - Fast discriminator circuits capable of triggering on low level pulses are being developed using tunnel diodes and transistors to obtain pulses of extremely short rise time and constant height. These will then be shaped by delay cables and will be used in conjunction with time-to-height converters to determine neutron energies precisely by measuring their time-of-flight with respect to a reference signal and also to measure short half-lives in the ns region.

4. <u>On the ion-optics of a split pole magnetic spectrograph</u> - M.N. Viswesvariah and N. Sarma - The ion-optics of a split pole magnetic spectrograph have been investigated theoretically. Expressions are derived for the final image distance, median plane and 'vertical' magnifications, dispersion, and momentum resolution. The effect of Doppler broadening due to nuclear reaction kinematics has also been taken into account. The equations were programmed for a CDC - 3600 computer and results obtained for a given pole face layout.

To be published in Nuclear Instrument and Methods.

---

* Tata Institute of Fundamental Research, Bombay.

5. <u>Current Integrator</u> - S.K. Gupta* - A transtorized current integrater has been designed to integrate currents ranging from 1 nA to 10 μA. The principle of the instrument is illustrated by the following block diagram:

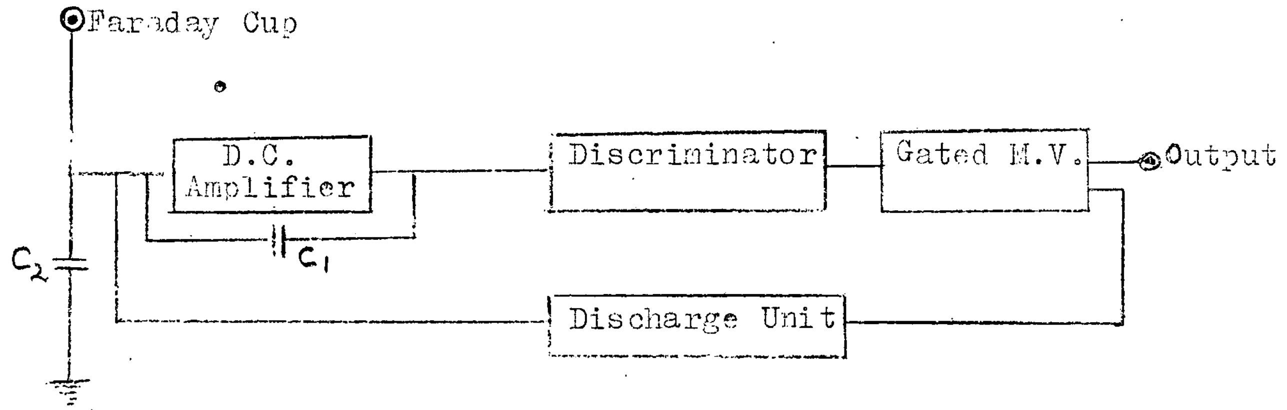

The condenser C_1 is charged using a D.C. amplifier. The rise of the voltage at the input is $\sim$1mV. When D.C. amplifier voltage reaches trigger level the discriminator actuates the multivibrator which in turn operates the discharge unit to remove a constant quantum of charge. The precision of the instrument is mostly dependent upon the constancy of discharge quantum.

The discharge unit consists of a transistor and two low leakage silcon diodes (IN3579) with a capacitor. The charging capacitor C_1 and the discharging capacitor have been chosen for very low leakage (Hermetically sealed silvered mica capacitors have proved to have lowest leakage). The capacitor C_2 quenches the voltage surges. The gated multivibrator provides occasional overload handling. The input leakage of the circuit is estimated to be $\sim 5 \times 10^{-12}$ amp. The circuit is being improved to increase

---

* Tata Institute of Fundamental Research, Bombay.

the range of currents handled and to improve the reliability of the circuit.

6. The ion optics of a generalized constant deviation magnetic spectrograph - M.N. Viswesvariah and N. Sarma - The problem of obtaining a third order focus in a constant deviation spectrograph has been treated analytically and a condition obtained giving rise to a number of possible combinations of incident angles E_1 and deviations $\emptyset$. One of the E_1, $\emptyset$ pairs of values agrees with the value used for a spectrograph built at Copenhagen[1]. For the other pairs of E_1, $\emptyset$ values, the first order ion optical parameters like final image distance, horizontal and vertical magnifications, momentum dispersion and resolution have been calculated. It is observed that the momentum resolution increases not only linearly with change in orbit radius a, but also with change in source distance, which makes it possible to obtain a desired resolution by a suitable change in source distance. A type of pole edge contouring used for the split-pole spectrograph[2], has been proposed for the constant deviation spectrograph also and the necessary changes in the equations for the calculation of vertical magnification have been taken into account.

1) Borggreen et al Nucl. Instr. & Methods 24 (1963) 1.

2) M.N. Viswesvariah and N. Sarma Nucl. Instr. & Methods (to be published).

RADIATION SURVEY

G. Muthukrishnan*

During the period under report ^{3}He beam was used for experiments in the Van de Graaff Accelerator. Fast neutron surveys were conducted at various places in the beam room and accelerator room. A B F_3 counter, surrounded with paraffin was used for the survey. It was calibrated with the standard 50 mc Ra-Be source and it was found to have a sensitivity of 2 cpm/unit neutron flux. The results of the survey are tabulated below:

Beam Room

^{3}He energy MeV	Beam current μa	Focus Pick-up μa	Bombarded material	Location	Fast neutron flux neutrons/ cm^2/sec.
2.5	0.15	0.9	V target	6 meters from the analysing magnet	20
2.5	0.15	0.9	V target	shielded entrance passage	8
2.5	0.15	0.9	V target	Outside beam room door	0
5.5	0.2	1.8	V target	6 meters from the analysing magnet	200
5.5	0.2	1.8	V target	shielded entrance passage	43
5.5	0.2	1.8	V target	outside beam room door	10

* Health Physics Division.

Accelerator Room

^{3}He energy MeV	Beam current μa	Focus pick-up μa	Bombarded material	Location	Fast neutron flux neutrons cm^2/sec.
2.5	0.15	0.9	V target	floor hatch	12
2.5	0.15	0.9	V target	Near the wall	0
2.5	0.15	0.9	V target	outside Accelerator room door	0
5.5	0.2	1.8	V target	floor hatch	60
5.5	0.2	1.8	V target	near the wall	40
5.5	0.2	1.8	V target	outside accelerator room door	0

SEMINARS

Weekly seminars were conducted in the Van de Graaff Laboratory. Personnel working on different problems gave interesting talks at these seminars. A series of lectures on 'Statistical analysis of the experimental data' were given by S.K. Gupta; Dr.A.S. Divatia and K.B. Nambiar dealt with High Vacuum Physics in a series of six lectures.

INDIAN NUCLEAR DATA GROUP

M. Balakrishnan (Secretary), H.J. Devare*, A.S. Divatia (Convener), D.N. Kundu**, B.P. Rastogi, M. Srinivasan and G. Venkataraman.

Information relevant to nuclear data collected from various institutions and laboratories has been compiled and published as the third progress report on Nuclear Data Measuring Activities in India. Copies of this report and other BARC reports of interest have been sent to the International Nuclear Data Committee (INDC) which is a part of the International Atomic Energy Agency, for international distribution.

Regular contributions were sent to the CINDA programme of the INDC. This programme involves scanning of all relevant Indian Journals and reports every month and sending the information regarding nuclear data contained in them in a specified CINDA-entry form.

The $^{16}O(n,\alpha)^{13}C$ reaction cross sections have been obtained from the $^{13}C(\alpha,n)^{16}O$ reaction, using the principle of reciprocity, in the incident neutron energy range 3.95 to 6.50 MeV. A paper on this was presented at the IAEA sponsored conference on Nuclear Data, held at Paris, during October 1966[1].

For accurate calibration of the 4π neutron counter a gas target set up for using the known reaction $D(d,n)^3He$ as the

---

* Tata Institute of Fundamental Research, Bombay
** Saha Institute of Nuclear Physics, Calcutta.

calibration reaction, was built. A manometer using a silicon oil as the liquid helps to measure the gas pressure and hence the target thickness very accurately.

All reports pertaining to nuclear data received from the IAEA are maintained separately in the Physics Group Library at Van de Graaff Laboratory, and are available for use. A list of these reports is prepared periodically and the list can be obtained on request.

1) A.S. Divatia, K.K. Sekharan and M.K. Mehta, The $^{16}C(n,\alpha)^{13}C$ Reaction Cross Sections from the $^{13}C(\alpha,n)^{16}O$ Reaction Cross Sections; To be published in the proceedings of the IAEA Conference on Nuclear Data-Microscopic Cross Sections and other Data Basic for Reactors, Paris, October 1966.

LIBRARY

The Physics Group Library at the Van de Graaff Laboratories registered a further growth during the year and is again experiencing a space shortage for the growing stock. A programme to assess the extent to which the computer can be used for processing the research reports in under study.

Library Collection: The library received 504 books and 235 bound volumes of periodicals during the year taking the total collection to 5037 volumes. This excludes B.A.R.C. reports and reprints which also registered an increase over the previous period.

Duplicate copies of research reports on Nuclear Physics and allied subjects received at the Depository library have been transferred to Van de Graaff Library during the year.

Micro film reader: A micro film reader has been installed in the library. Steps to convert it into a micro-fiche reader which is found to be more of use, is under consideration.

Library Guide: A pamphlet "A Guide for users of Van de Graaff Library" is under preparation. It is proposed to issue cyclo-styled copies of this pamphlet to the library users.